forests

MDPI

Article

Transcriptomic and Anatomic Profiling Reveal Etiolation Promotes Adventitious Rooting by Exogenous Application of 1-Naphthalene Acetic Acid in *Robinia pseudoacacia* L.

Muhammad Zeeshan Munir [1,†], Saleem Ud Din [1,†], Muhammad Imran [2], Zijie Zhang [1], Tariq Pervaiz [3], Chao Han [1], Zaib Un Nisa [4,5], Ali Bakhsh [6], Muhammad Atif Muneer [7], Yuhan Sun [1] and Yun Li [1,*]

1 Beijing Advanced Innovation Center for Tree Breeding by Molecular Design, National Engineering Laboratory for Tree Breeding, Robinia pseudoacacia Engineering Technology Research Center of National Forestry and Grassland Administration, College of Biological Science and Technology, Beijing Forestry University, Beijing 100083, China; zeeshanmunir1270@gmail.com (M.Z.M.); saleemkhan86@hotmail.com (S.U.D.); zijiezhang@bjfu.edu.cn (Z.Z.); jiani.690@163.com (C.H.); syh831008@163.com (Y.S.)
2 State Key Laboratory of Plant Cell and Chromosome Engineering, Institute of Genetics and Developmental Biology, Chinese Academy of Sciences, Beijing 100101, China; imran_m1303@yahoo.com
3 Beijing Advanced Innovation Center for Tree Breeding by Molecular Design, Beijing Forestry University, Beijing 100083, China; tariqzoqi2009@gmail.com
4 College of Biological Sciences and Technology, Beijing Forestry University, Beijing 100083, China; zaibsci.agri@gmail.com
5 Cotton Research Institute Multan, Multan 60000, Pakistan
6 Department of Plant Breeding and Genetics, Ghazi University, Dera Ghazi Khan 32200, Pakistan; abakhsh@gudgk.edu.pk
7 International Magnesium Institute, College of Resources and Environment, Fujian Agriculture and Forestry University, Fuzhou 350002, China; m_atifmuneer@yahoo.com
* Correspondence: yunli@bjfu.edu.cn; Tel.: +86-10-6233-6094
† These authors contributed equally to this article.

Abstract: The process of etiolation contributes significantly to vegetative propagation and root formation of woody plants. However, the molecular interaction pattern of different factors for etiolated adventitious root development in woody plants remains unclear. In the present study, we explored the changes at different etiolation stages of adventitious root formation in *Robinia pseudoacacia*. Histological and transcriptomic analyses were performed for the etiolated lower portion of hypocotyls to ascertain the adventitious root responses. We found that the dark-treated hypocotyls formed roots earlier than the control. Exogenous application of NAA (0.3 mg/L) stimulated the expressions of about 310 genes. Among these, 155 were upregulated and 155 were downregulated. Moreover, differentially expressed genes (DEGs) were significantly enriched in multiple pathways, including the biosynthesis of secondary metabolites, metabolic pathway, plant hormone signal transduction, starch and sucrose metabolism, phenylpropanoid biosynthesis, and carbon metabolism. These pathways could play a significant role during adventitious root formation in etiolated hypocotyls. The findings of this study can provide novel insights and a foundation for further studies to elucidate the connection between etiolation and adventitious root formation in woody plants.

Keywords: histology; RNA-sequencing; in vitro; multiple pathways; auxin; expression profile; black locust; rooting stages; dark pretreatment

Citation: Munir, M.Z.; Ud Din, S.; Imran, M.; Zhang, Z.; Pervaiz, T.; Han, C.; Un Nisa, Z.; Bakhsh, A.; Atif Muneer, M.; Sun, Y.; et al. Transcriptomic and Anatomic Profiling Reveal Etiolation Promotes Adventitious Rooting by Exogenous Application of 1-Naphthalene Acetic Acid in *Robinia pseudoacacia* L. *Forests* **2021**, *12*, 789. https://doi.org/10.3390/f12060789

Academic Editors: Tadeusz Malewski and Carol A. Loopstra

Received: 16 March 2021
Accepted: 10 June 2021
Published: 15 June 2021

1. Introduction

R. pseudoacacia is native to North America and was first introduced to China in 1877 [1]. *R. pseudoacacia* possesses the most significant ecological and economic characteristics, including excellent coppicing, fast growth, high yield, and adaptability to a wide range of environments [2]. Several reports have shown that in vitro propagation of *R. pseudoacacia* is an effective method to produce large numbers of clonal plants [3] because woody species

are usually more difficult to root than herbaceous plants [4]. Thus, the low rooting rate is a limiting and crucial factor of *R. pseudoacacia*, making it difficult to grow in a variety of environments [5]. However, it has been found that different stresses such as wounding, etiolation, and the application of phytohormones have a significant effect on adventitious root formation [6]. Three major factors, including light/dark, phytohormones, and nitrogen oxide, have been recognized to induce adventitious root formation [7]. Therefore, understanding the formation of adventitious roots through potential factors, including etiolation and phytohormones, is a matter of great interest to offset the rooting problem in *R. pseudoacacia*.

Partial or complete darkness for a specific time period is termed as etiolation [8]. It improves the rooting ability of cuttings [9]. Etiolation is an effective method that promotes vegetative propagation in woody and herbaceous plants. It increases the number of shoots, the elongation of shoots, and the rate of nodal regeneration. Under optimum conditions, darkness as a pretreatment increases root formation and also increases the number and length of roots [9]. In *Tectona grandis*, etiolation as a pretreatment promotes shoot length and shoot number and also improves the number, length, and percentage of root formation [9]. The interaction between etiolation and phytohormones could be an important source of adventitious rooting.

Phytohormones counteract the adventitious root formation using various external and internal stimuli such as etiolation and wounding [10]. Auxin is the most important growth regulator to trigger adventitious root initiation. High auxin levels are required in the basal region of cuttings in many plant species, which may help in the initiation and proliferation of many tissues in cambium layers for adventitious rooting [11]. A higher level of auxin is important during the induction phase to reprogram the fate of cells and tissues. In contrast, a lower level of auxin is required to allow organogenesis [12]. Other hormones, including ethylene, cytokinin, salicylic acid, brassinosteroids, and jasmonic acid, act to channelize the process of adventitious root formation [13]. Ethylene has a significant role in adventitious root formation and the elongation of etiolated plant organs [14], and the free movement of carbohydrates from starch [15]. Synthetic auxin, including indole-3-butyric acid (IBA) and 1-naphthalene acetic acid, is applied exogenously to promote adventitious root formation [16]. NAA promotes root formation [17]. Previous studies have identified a few auxin genes (*AUX/IAA*, *PtRR13*, *AP2/ERF*, *GH3*, *PIN*, *AIR3*) that regulate the adventitious root formation in woody species [18]. They play a significant role in adventitious root formation during the process of embryogenesis [19]. However, the potential role of NAA in adventitious rooting has not been fully explored.

With the above in mind, adventitious root formation is a limiting factor in the vegetative propagation of *R. pseudoacacia* and other tree species as well. Unfortunately, the molecular mechanism underlying adventitious root formation remains unclear, and especially the mechanism of etiolation is scarce. Thus, the current study was conducted to control the adventitious root formation in etiolated hypocotyls of *R. pseudoacacia*. The key objectives of this study were: (1) to investigate the histological changes of adventitious root formation; (2) to elucidate the molecular mechanism for adventitious root formation; and (3) to identify the genes involved in enriched pathways. High throughput sequencing analysis was conducted to monitor the global changes occurring at the gene expression levels during adventitious root formation in *R. pseudoacacia.*

2. Results

2.1. Histological Changes for the Process of Adventitious Root Formation in R. pseudoacacia

R. pseudoacacia-148 seeds were chosen for this study due to their relatively better rooting performance than other clones and differential response to a mild NAA treatment during adventitious root formation (Figure 1).

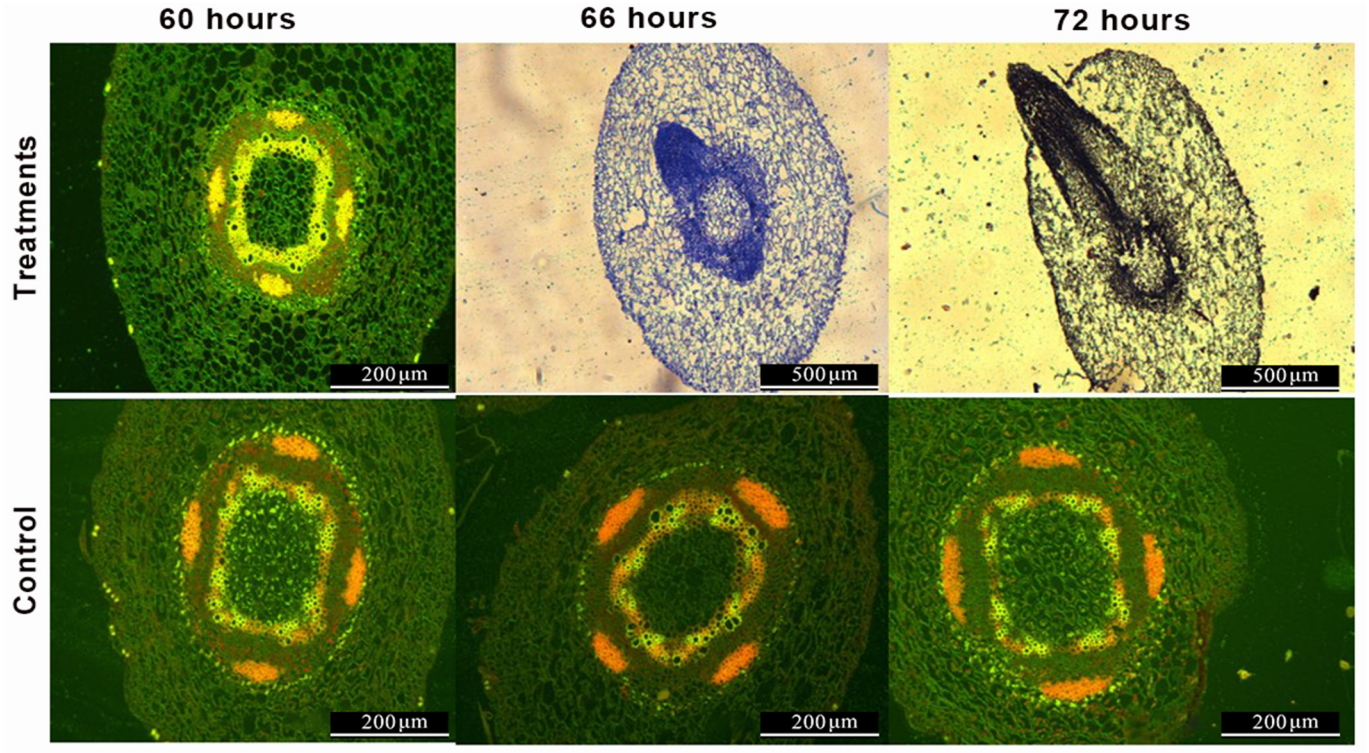

Figure 1. Anatomical structure of adventitious root formation over time in the hypocotyl of *R. pseudoacacia*. Three developmental stages were observed at 60 h, 66 h, and 72 h for control and treatment with NAA application. Control did not exhibit any change at tested time points but donor treated showed significant changes at three tested time points. At 60 h small cells started division near vascular bundles and gathered to form adventitious roots at 66 h and at 72 h. The scale bar for pictures of the control was 200 µm. For treatment, only 60 h was at 200 µm but the other two time points (66 h, 72 h) were 500 µm.

Under NAA treatment, the *R. pseudoacacia*-148 hypocotyl developed a small callus and exhibited root elongation at 72 h in donor-treated plants. In the control, *R. pseudoacacia*-148 did not exhibit any change during tested stages of adventitious root formation (Figure 1). Under NAA treatment, the histology at 60 h (2.5 days), 66 h (2.75 days), and 72 h (3 days) showed obvious changes (Figure 1), but under the control conditions, the hypocotyl tissues up to 72 h did not exhibit any change. At each time point (60 h, 66 h, and 72 h), there was a clear difference between the treatment and control. The small callus was formed on the wounded sites of the hypocotyl in culturing medium at 72 h. Furthermore, the gathering of cells and division was initiated at 60 h, a dome-shaped adventitious root primordium was visible at 66 h, and root emergence from the hypocotyl was recorded at 72 h (Figure 1). Based on the histological observations, adventitious root formation indicated that dark pretreatment had boosted up the root formation as compared to the control. Anatomical visualization for transcriptome analysis was used to validate the accuracy of the sampling time point. These anatomical observations provide basic information about adventitious root formation in *R. pseudoacacia*.

2.2. Deep Sequencing, Functional Annotation of DEGs, and qRT-PCR Analysis

A total of six samples generated 38–60 million clean reads. On average, 7.72 Gb of data was produced (Table 1). For all sequenced data, the Q30 percentage was greater than 91% (Table 1). The final mapping result of tested reads against a reference (*R. pseudoacacia*) was about 85.89% (Table 1). After reference genome alignment, a total of 45,164 new transcripts were found, out of which 29,472 belonged to a novel isoform, 4042 transcripts belonged to the new protein-coding genes, 33,514 were coding transcripts, while the remaining 11,650 were long-chain non-coding RNAs. On average, 24,488 genes were detected per sample by comparing reads to genes, using the "bowtie2" software. For differential gene

analysis, an average of 310 genes were detected, in which 155 were upregulated and 155 were downregulated. The distribution intervals of gene expression level in RNA-seq data of each sample are shown in Figure S1.

Table 1. Statistical summary of RNA-sequencing libraries.

Sample	Clean Reads (M)	Clean Bases (G)	Q20 (%)	Q30 (%)	GC (%)	Read Length (bp)	Total Mapped (%)	Splice Mapped (%)	Unique Mapped (%)	Multiple Mapped (%)
BL-CK60-R1	41.6759	6.2514	96.95%	91.80%	42.63%	150	86.44%	30.60%	81.60%	4.84%
BL-CK60-R2	40.7821	6.1275	97.54%	93.07%	42.20%	150	87.42%	30.56%	82.88%	4.54%
BL-CK60-R3	39.9473	5.9921	96.85%	91.62%	42.95%	150	86.87%	32.51%	82.23%	4.64%
BL-60-R1	46.7699	7.0155	96.82%	91.56%	42.38%	150	85.98%	30.32%	81.73%	4.24%
BL-60-R2	45.0371	6.7556	96.68%	91.25%	42.39%	150	84.91%	28.39%	80.41%	4.50%
BL-60-R3	59.2106	8.8816	97.78%	93.59%	42.35%	150	84.75%	26.66%	80.59%	4.16%
BL-66-R1	38.8345	5.8252	96.85%	91.55%	42.43%	150	86.52%	29.99%	81.83%	4.69%
BL-66-R2	41.0296	6.1544	96.97%	91.81%	42.11%	150	86.20%	28.55%	81.68%	4.51%
BL-66-R3	41.4342	6.2151	96.88%	91.62%	42.46%	150	87.36%	31.33%	82.67%	4.69%
BL-72-R1	57.8766	8.6815	97.34%	92.74%	42.23%	150	82.91%	26.06%	78.76%	4.15%
BL-72-R2	47.1213	7.0682	96.87%	91.69%	42.30%	150	83.40%	25.65%	79.24%	4.17%
BL-72-R3	47.6405	7.1461	96.79%	91.47%	42.43%	150	84.22%	27.69%	79.91%	4.31%

Note: Where BL-CK60 is sample of Black Locust under control at 60 h, BL-60 is sample of Black Locust under etiolation at 60 h, BL-66 is sample of Black Locust under etiolation at 66 h, BL-72 is sample of Black Locust under etiolation at 72 h, Q20% and Q30% are the percentages of bases with a Phred value greater than 20 and 30 as a percentage of the total base, respectively. GC% is GC content in percentage.

In the present study, DEGs were analyzed among different comparisons of treatment and with their respective control at 60 h (CK60). There were 12, 51, and 383 DEGs in a total and 4, 51, and 367 specific DEGs between the control and treatment, respectively (Figure 2a), and 142, 341, and 580 DEGs and 60, 151, and 349 specific DEGs among treatments were found (60 h, 66 h, and 72 h) (Figure 2b). Meanwhile, 4, 17, and 216 upregulated genes and 8, 46, and 167 downregulated genes were recorded between the control and treatment, respectively (Figure 2c). Among the treated samples (60 h, 66 h, 72 h), 57, 212, and 378 upregulated genes and 85, 129, and 202 downregulated genes were expressed at each time point, respectively (Figure 2c). Furthermore, principal component analysis (PCA) showed that the BL-60 group was in the same quadrant, and two replications of each sample were in the same quadrant in BL-60, BL-72, and BL-CK60 (Figure S2b). Almost all groups were closely associated with each other, which shows a strong correlation (Figure S2a). A heat map of all DEGs on a selected time point is presented in Figure 2d.

Gene ontology (GO) assignment was performed to classify the functions of DEGs at different time points (60 h, 66 h, and 72 h) (Figure S3, Table S1). The DEGs between the control and treatment were categorized into different comparisons (BL-CK60-VS-BL-60: 18, 13, 13), (BL-CK60-VS-BL-66: 153, 152, 64), (BL-CK60-VS-BL-72: 730, 549, 346) (Figure S3a–c) and among treatments (BL-60-VS-BL-66: 236, 257, 127), (BL-60-VS-BL-72: 553, 393, 269) and (BL-66-VS-BL-72: 1036, 825, 507) (Figure S3d–f), divided into the biological process, cellular component, and molecular function, respectively. Most DEGs were assigned to metabolic process, cellular process, biological regulation, and response to stimulus in the category of biological process; cell part, cell, and membrane in the category of cellular component; and binding, catalytic activity, and transporter activity in the category of molecular function (Figure S3). Within the biological category, GO terms of DEGs including metabolic process (GO:0008152), cellular process (GO:0009987), single-organism process (GO:0044699), and biological regulation (GO:0065007) were significantly enriched (Figure 3).

To further elaborate the biological interpretation, all DEGs were mapped to the KEGG database (Figure 4, Table S2). According to KEGG pathway enrichment analysis, 10, 66, and 353 DEGs were classified into 10, 14, and 20 pathways in BL-CK60-vs-BL-60, BL-CK60-vs-BL-66, and BL-CK60-vs-BL-72 comparisons, respectively (Figure 4a–c), and 120, 302 and 491 DEGs were classified into 18, 19, and 20 pathways in BL-60-vs-BL-66, BL-60-vs-BL-72, and BL-66-vs-BL-72, respectively (Figure 4d–f). The annotated changes were mainly enriched in pathways such as the metabolic pathway, biosynthesis of secondary metabolites, carbon metabolism, plant hormone signal transduction, phenylpropanoid biosynthesis, and also starch and sucrose metabolism (Figure 5).

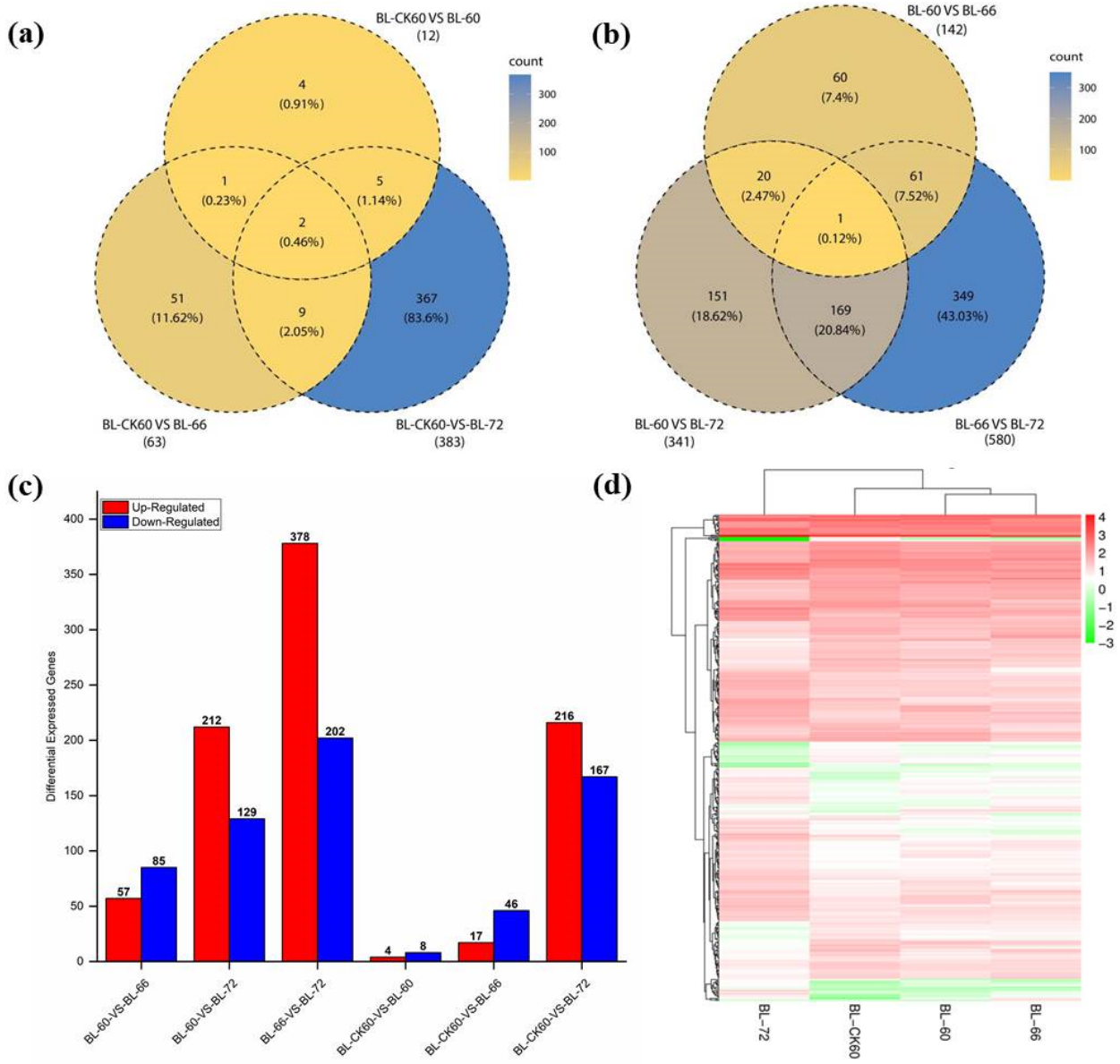

Figure 2. DEGs control vs. treatment and among treatment comparisons at 60 h, 66 h, and 72 h tested time points; (**a**) DEGs between control and treatment comparison at three tested time points (60 h, 66 h, 72 h); (**b**) DEGs among treatment comparisons at three time points (60 h, 66 h, 72 h); (**c**) Histogram representing the number of upregulated and downregulated DEGs; (**d**) Clustering heat map of all DEGs at 60 h, 66 h, and 72 h.

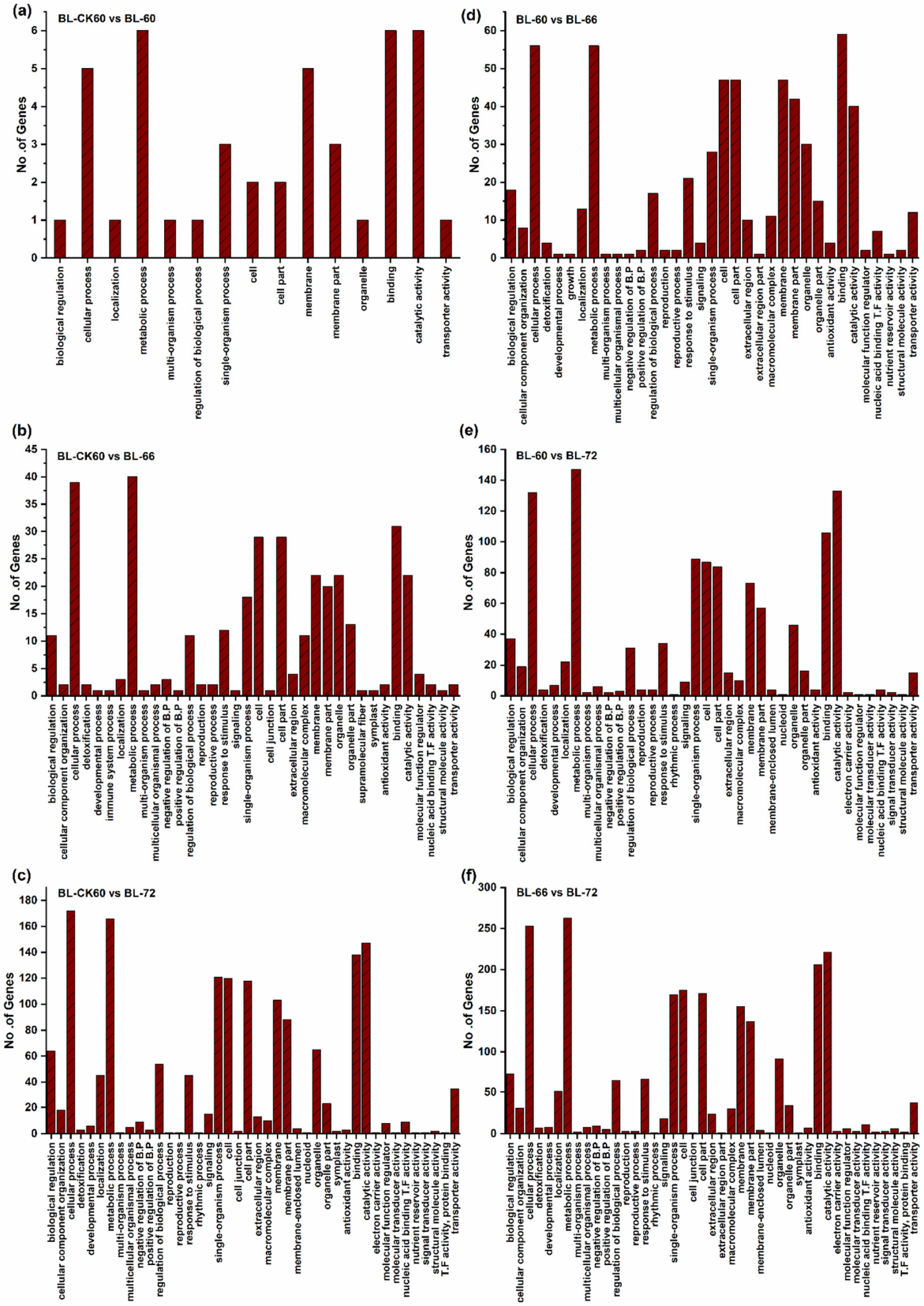

Figure 3. Biological process analysis of DEGs between control and treatment, and among treatments at three tested time points (60 h, 66 h, and 72 h); (**a**–**c**) Biological process analysis of DEGs between control and treatment at tested time points (60 h, 66 h, 72 h); (**d**–**f**) Biological process analysis of DEGs among treatment comparisons at tested time points (60 h, 66 h, 72 h).

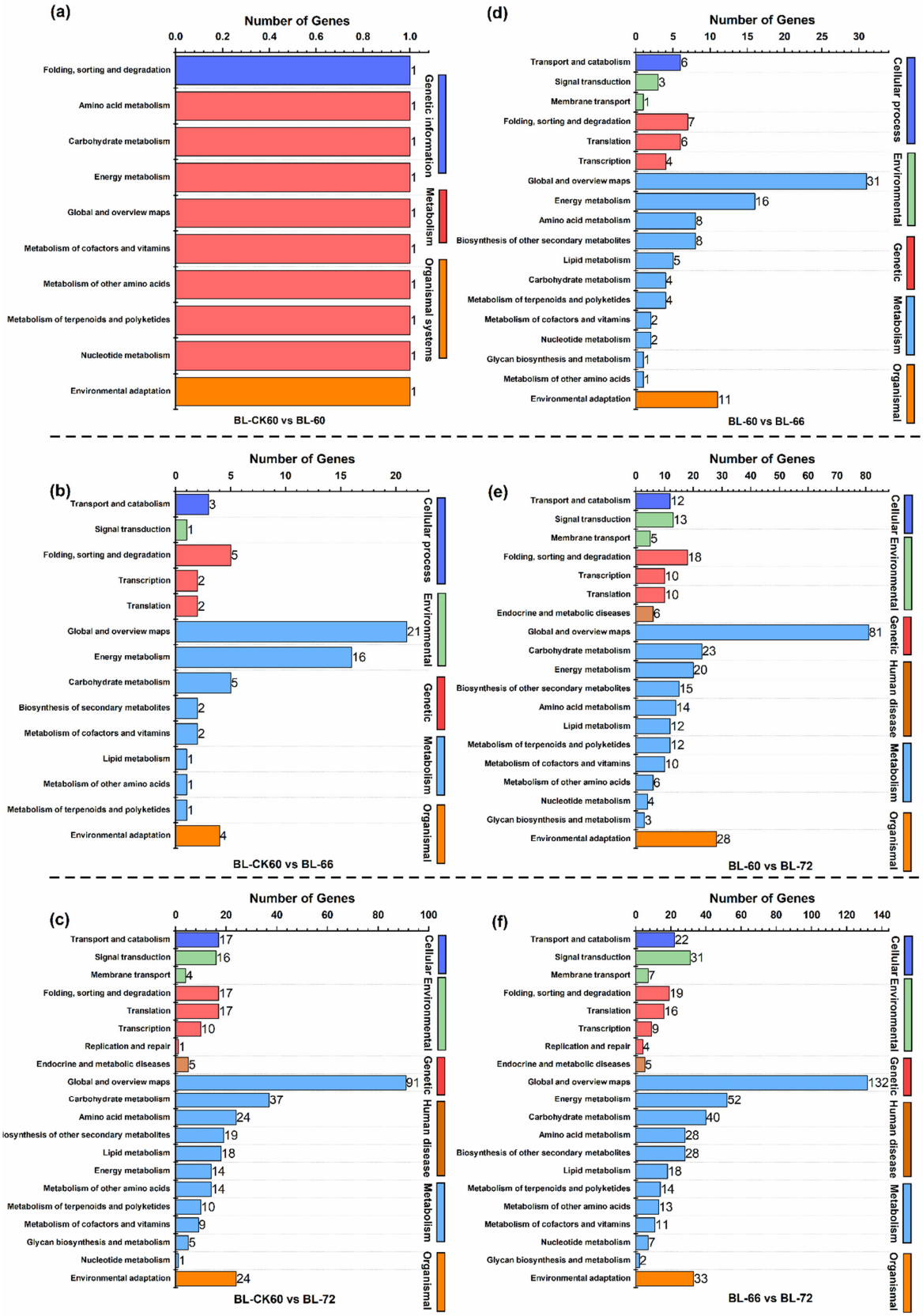

Figure 4. KEGG pathway classification of DEGs between control and treatment and among treatments at three tested time points (60 h, 66 h, and 72 h); (**a–c**) KEGG pathway classification of DEGs between control and treatment at tested time points (60 h, 66 h, 72 h); (**d–f**) KEGG pathway classification of DEGs among treatment comparisons at tested time points (60 h, 66 h, 72 h).

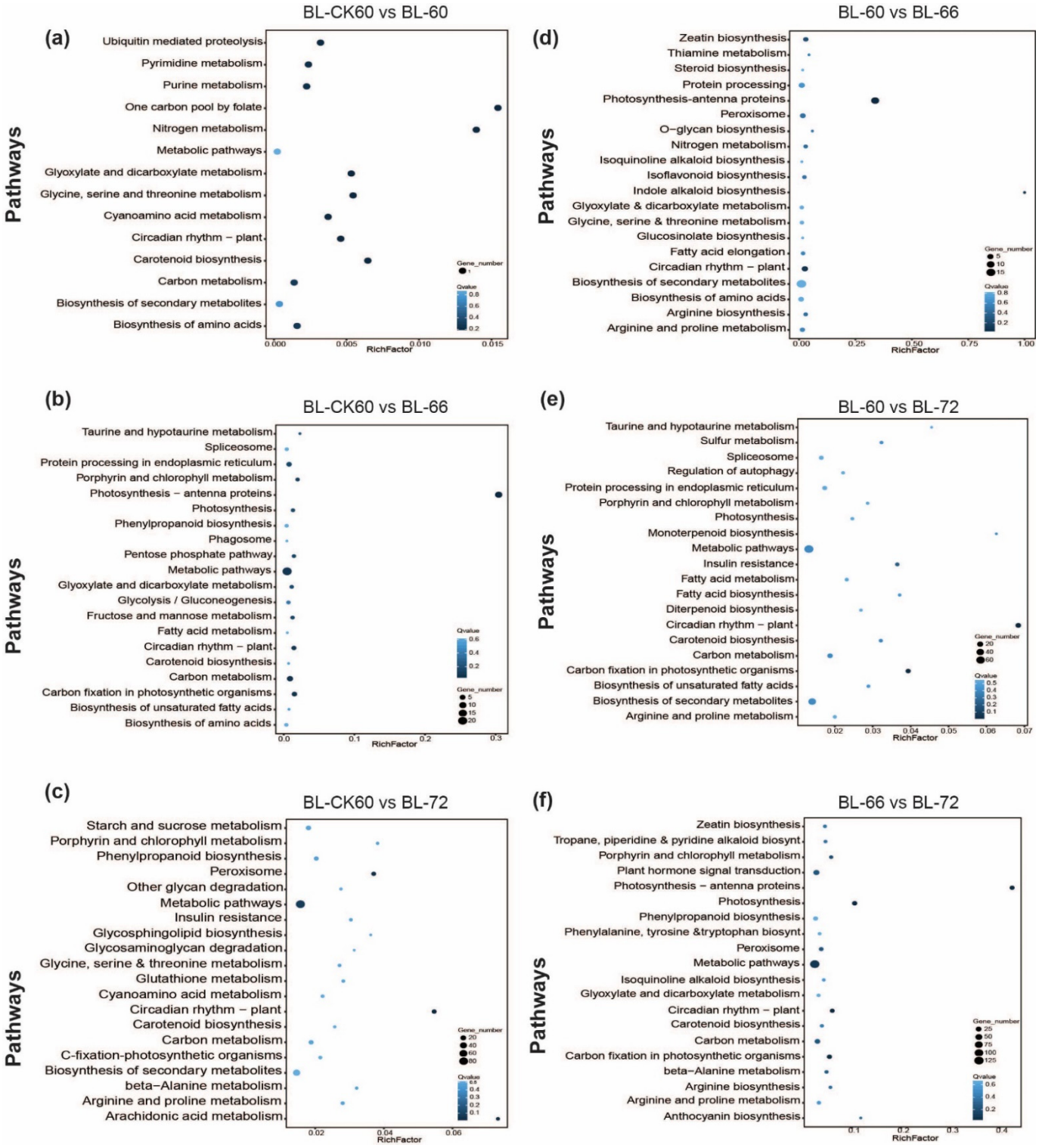

Figure 5. Top 20 KEGG pathway enrichments of DEGs between control and treatment and among treatments at three tested time points (60 h, 66 h, and 72 h); (**a**–**c**) Top 20 KEGG pathway enrichments of DEGs between control and treatment at tested time points (60 h, 66 h, 72 h); (**d**–**f**) Top 20 KEGG pathway enrichments of DEGs among treatment comparisons at tested time points (60 h, 66 h, and 72 h).

2.3. *Effect of Exogenous NAA on Plant Hormone Signal Transduction Pathway*

Transcriptome analysis revealed differentially expressed genes related to phytohormones, cytokinin, auxin, jasmonic acid, brassinosteroids, gibberellin, and salicylic acid.

Phytohormones play important roles in the regulation of adventitious root formation. In the present study, the auxin signaling pathway genes (*AUX/IAA*, *SAUR*, and *GH3*), cytokinin signaling genes (*B-ARRs*, *APL*, and *EFM*), abscisic acid-related genes (*PP2C*, *SNRK2-7* and *ABI5*), salicylic acid signaling genes, jasmonic acid, brassinosteroids (*MYC2*, *TCH4*, *BRI1*, *SPL12*, *TGA9*, and *PR-1-LIKE*), and gibberellin-related *SCL15* gene were identified. These genes exhibited changes in expression levels at various stages of adventitious root formation at 60 h, 66 h, and 72 h. A heat map of all DEGs related to hormones on FPKM $\log_2$ fold values and their relative qRT-PCR is presented (Figure 6, Table S3).

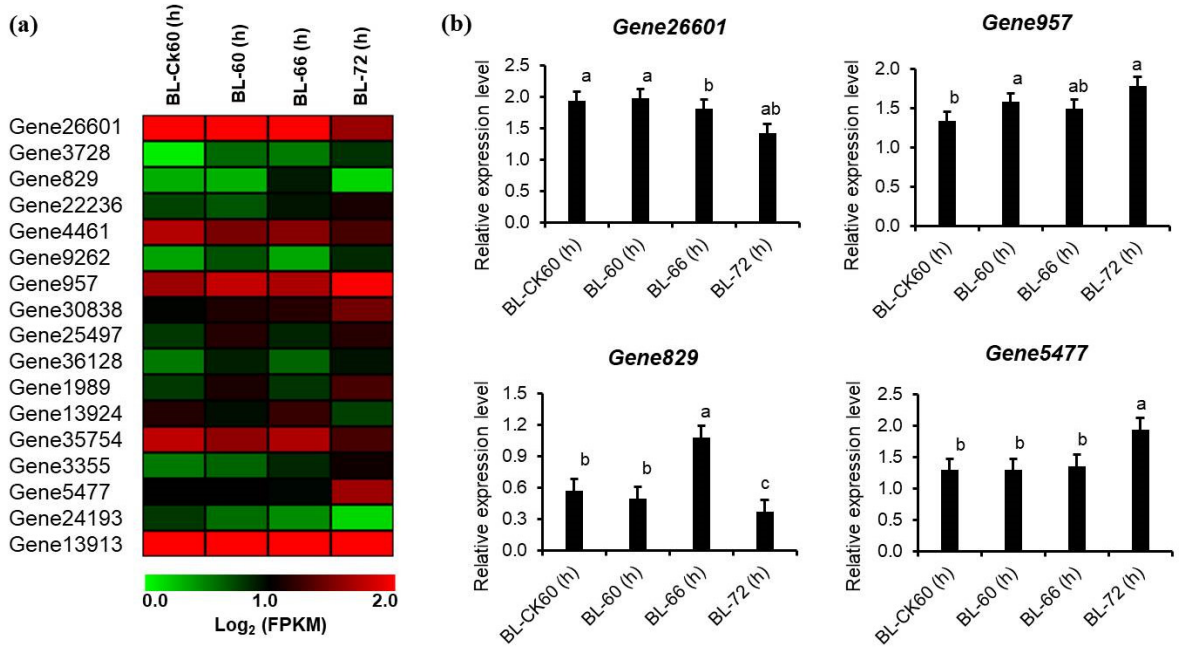

Figure 6. Expression profiling of plant hormone signal transduction DEGs in the hypocotyl of *R. pseudoacacia*-148 during adventitious root formation; (**a**) Heat map illustration of log2 (FPKM) values for annotated genes during hormone signal transduction pathway; (**b**) Relative expression of hormone transduction pathway genes as determined by RT-qPCR. The data presented are the average of three technical replicates. Different letters indicate significant difference by least significant difference (LSD) test ($p \leq 0.05$). Bar = SD.

2.3.1. Auxin

The heat map of DEGs is presented in Figure 6a. In the present study, exogenous NAA treatment upregulated the relative expression of auxins, *AUX/IAA*; *indole-3-acetic acid-inducible 19* (gene26601), which decreased from BL-60 h to BL-72 h (Figure 6b). The expression of the *SAUR* (gene3728) gene decreased from BL-60 h to BL-66 h and then increased from BL-66 h to BL-72 h (Table S3). In contrast, *GH3.3* (gene829) was upregulated from BL-60 h to BL-66 h and decreased from BL-66 h to BL-72 h (Figure 6b). The qRT-PCR data showed that an exogenous NAA application induced auxin-related gene expression compared to the control (Figure 6).

2.3.2. Cytokinin

The relative expressions of cytokinin and two pseudo-response regulators 2(*PRR2*) were observed under the NAA treatment. The expression of *PRR2* (gene957) first decreased then increased from BL-60 h to BL-72 h (Figure 6b), while the expression of *PRR2* (gene30838) continuously increased from BL-60 h to BL-72 h (Table S3). The expression of another two genes, altered phloem development (*APL*) (gene25497) and early flowering myb protein (*EFM*) (gene36128), first decreased then increased from BL-60 h to BL-72 h (Table S3).

2.3.3. Abscisic Acid

The relative expression of abscisic acid, protein phosphatase 2CA *(PP2C*, gene22236) continuously increased from BL-60 h to BL-72 h under NAA treatment. The *SNF1*-related protein kinase 2–7(*SNRK2-7*, gene4461) first increased then decreased from BL-60 h to BL-72 h. Abscisic acid insensitive 5 (*ABI5*, gene9262) expression decreased from BL-60 h to BL-66 h and increased from BL-66 h to BL-72 h (Table S3).

2.3.4. Gibberellic Acid

There are relatively few studies on GA-regulated root development in woody plants. *DELLA*, scarecrow-like 15 (*SCL15*) (gene1989) has been found with decreasing expression to increasing expression from BL-60 h to BL-72 h (Table S3).

2.3.5. Jasmonic Acid, Brassinosteroids, and Salicylic Acid

In the present study, jasmonic acid genes such as *MYC2* genes (gene13924, gene35754), brassinosteroids *TCH4* (xyloglucan endo trans glycosylase 6; gene5477) and *BRI1* (squamosa promoter-binding protein-like 12) (*SPL12*; gene3355), pathogenesis-related gene 1 (*PR1*; gene13913), and *TGA9* (gene24193) were differentially expressed during adventitious root formation. Under NAA treatment, the relative expression of jasmonic acid-related genes, (*MYC2*; gene13924) and (*MYC2*; gene35754), first increased and then decreased from BL-60 h to BL-72 h (Table S3). The relative expression of brassinosteroid genes, (*SPL12*; gene3355) and (*TCH4*; gene5477), was found. The expression of the first gene increased continuously from BL-60 h to BL-72 h (Table S3). The second gene's expression first decreased and then increased from BL-60 h to BL-72 h (Figure 6b). The relative expression of salicylic acid, motif-binding protein 9 (*TGA9*) (gene24193) expression continuously decreased from BL-60 h to BL-72 h (Table S3). The expression of pathogenesis-related protein-1-like (*PR-1-LIKE*) (gene13913) first increased and then decreased from BL-60 h to BL-72 h (Table S3).

2.3.6. Starch and Sucrose Metabolism Pathway

The initiation and development of the adventitious root primordium require more energy triggered by starch, which is a significant source of carbohydrates in woody plants [20]. The heat map of differentially expressed genes (DEGs) and qRT-PCR are presented in Figure 7a. Under NAA treatment, the relative expression level of *SUS3* (gene9499) slightly increased from BL-60 h to BL-72 h. In contrast, AIR3 (gene30616) expression continuously decreased from BL-60 h to BL-72 h (Figure 7b). Three genes of the plant invertase/pectin methyl esterase inhibitor superfamily were found. Two genes showed opposite trends. Gene19401 continuously increased from BL-60 h to BL-72 h, and gene1053 continuously decreased from BL-60 h to BL-72 h (Table S3). Gene198 first decreased from BL-60 h to BL-66 h and then increased from BL-66 h to BL-72 h (Table S3). Gene17148 showed slightly decreasing expression trends, and while the gene1118 downregulated from BL-60 h to BL-66 h and then upregulated from BL-66 h to BL-72 h (Table S3), respectively. In addition, *BMY5* (gene15899) showed an increasing trend from BL-60 h to BL-66 h and then decreased from BL-66 h to BL-72 h (Figure 7b). RT-qPCR also validated the expression pattern of selected genes. Under NAA treatment, most of the expression profiles for the aforementioned genes were consistent with the profiles obtained by RT-qPCR (Figure 7).

2.3.7. Phenylpropanoid Biosynthesis Pathway

Heat maps of all DEGs expressed during phenylpropanoid biosynthesis were examined during the three tested time points (60 h, 66 h, 72 h) (Figure 8a) of adventitious root formation, which were all upregulated. Among phenylpropanoid DEGs, *Arabidopsis thaliana* peroxidase *CB* (gene5) expression increased continuously from BL-60 h to BL-72 h (Figure 8b). In addition, peroxidase superfamily protein (gene12931) (Figure 8b) and peroxidase 2 (gene12930) showed a similar trend, first increasing from BL-60 h to BL-66 h and then decreasing from BL-66 h to BL-72 h (Table S3). Contrarily, the expression of two genes, peroxidase 40 (gene22473) (Figure 8b) and telomeric DNA-binding protein

2 (gene22265), increased continuously from BL-60 h to BL-72 h (Table S3). Most of the expression profiles for the aforementioned genes were consistent with the profiles obtained by RT-qPCR (Figure 8).

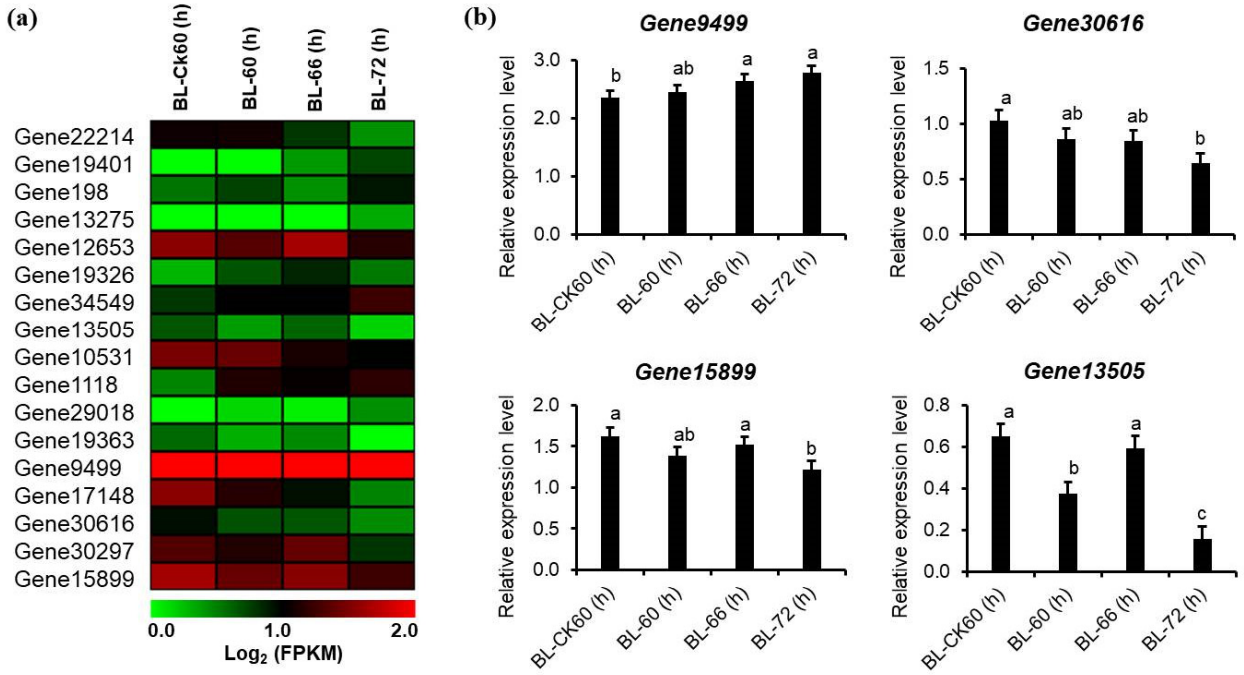

Figure 7. Expression profiling of starch and sucrose metabolism DEGs in the hypocotyl of *R. pseudoacacia*-148 during adventitious root formation; (**a**) Heat map illustration of log2 (FPKM) values for annotated genes during starch and sucrose metabolism pathway; (**b**) Relative expression of starch and sucrose metabolism pathway genes as determined by RT-qPCR. The data presented are the average of three technical replicates. Different letters indicate significant difference by least significant difference (LSD) test ($p \leq 0.05$). Bar = SD.

2.3.8. Carbon Metabolism Pathway

The heat map of all DEGs involved in carbon metabolism is presented in Figure 9a, and carbon metabolism is an essential pathway in plants for the production of structural components and energy sources. DEGs expressed in carbon metabolism might be playing a plausible role during adventitious root formation. These genes included *PSAT1* (phosphoserine aminotransferase 1), *SERAT3;2* (serine acetyltransferase 3;2), *GOX1* (glycolate oxidase 1), *FBA1* (fructose-bisphosphate aldolase 1), *PFK7* (phosphofructokinase 7), *PRK* (phosphoribulokinase) and *SHM1* (serine hydroxy methyltransferase 1). With NAA treatment, the relative expression level of GOX1 (gene25254), FBA1 (gene16722), and PFK7 (gene23954) first decreased from stage BL-60 h to BL-66 h and then increased from stage BL-66 h to BL-72 h, and the expression of the first two genes was observed at BL-72 h and for the last one at BL-60 h, respectively (Figure 9b). The relative expression continuously increased from BL-60 h to BL-72 h in the case of *SERAT3;2* (gene2215) (Figure 9b) and *PRK* (gene30172) (Table S3), with the highest expression at BL-72 h. *PSAT1* (gene30347) exhibited an increasing trend from BL-60 h to BL-66 h and then decreased from BL-66 h to BL-72 h (Table S3). Most of the above-mentioned genes showed positive expression, but *SHM1* (gene30059) showed negative expression at 60 h and 66 h and then changed to positive expression at 72 h (Figure 9a). Collectively, the RT-qPCR results indicated that the relative expression levels of carbon metabolism-related genes were affected by the exogenous NAA application compared to the control, while results were consistent with RNA-sequencing (Figure 9).

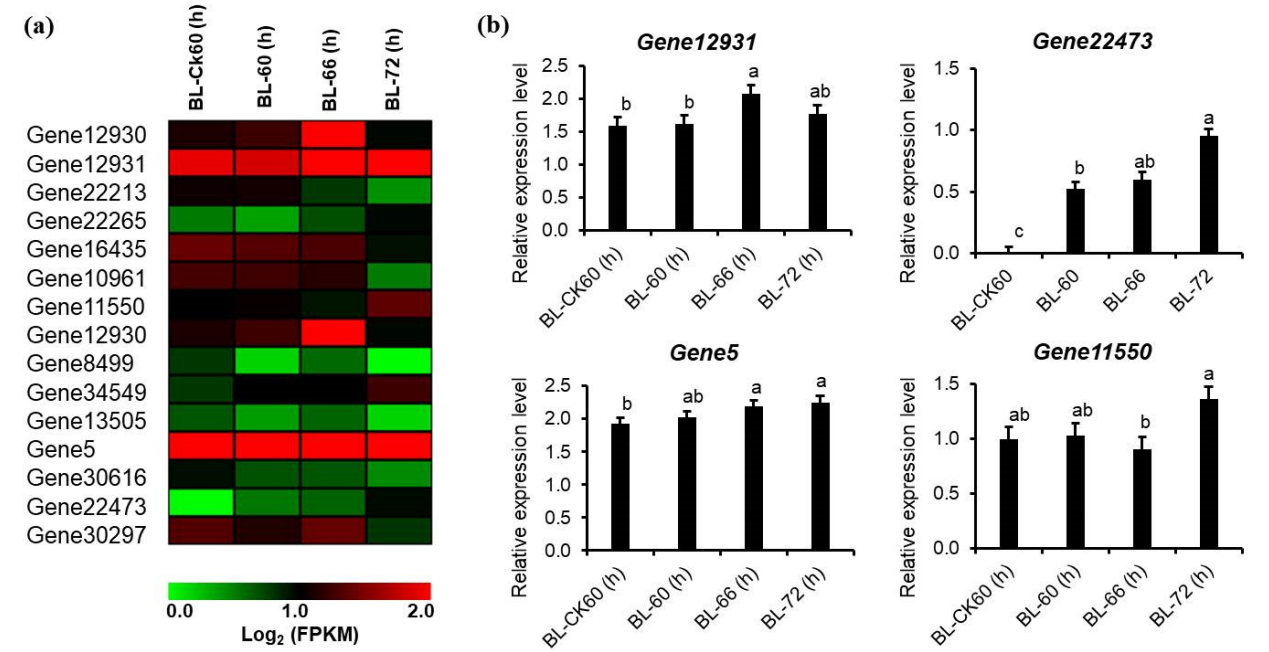

Figure 8. Expression profiling of phenylpropanoid biosynthesis DEGs in the hypocotyl of *R. pseudoacacia*-148 during adventitious root formation; (**a**) Heat map illustration of log2 (FPKM) values for annotated genes during phenylpropanoid biosynthesis pathway; (**b**) Relative expression of phenylpropanoid biosynthesis pathway genes as determined by RT-qPCR. The data presented are the average of three technical replicates. Different letters indicate significant difference by least significant difference (LSD) test ($p \leq 0.05$). Bar = SD.

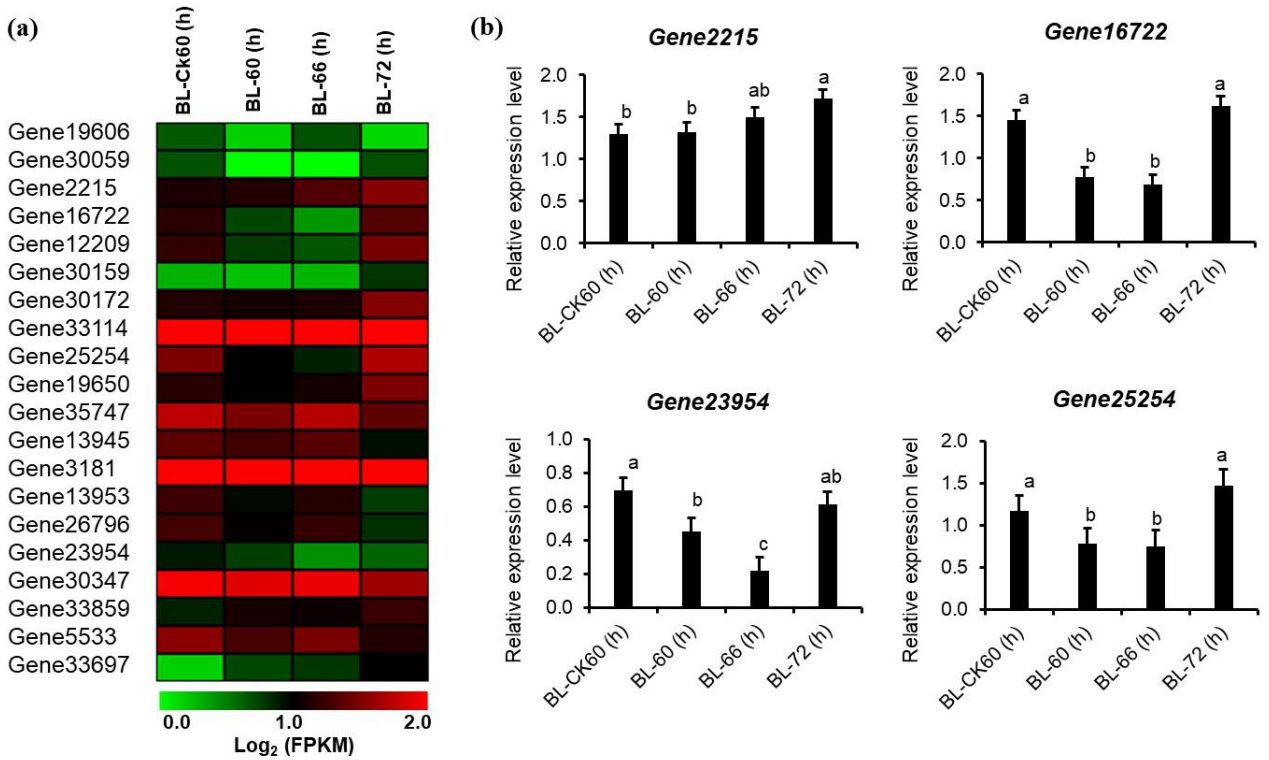

Figure 9. Expression profiling of carbon metabolism DEGs in the hypocotyl of *Robinia pseudoacacia*-148 during adventitious root formation; (**a**) Heat map illustration of log2 (FPKM) values for annotated genes during carbon metabolism pathway; (**b**) Relative expression of carbon metabolism pathway genes as determined by RT-qPCR. The data presented are the average of three technical replicates. Different letters indicate significant difference by least significant difference (LSD) test ($p \leq 0.05$). Bar = SD.

3. Discussion

Since antiquity, root formation has been improved by propagating avocado stock plants in darkness [21,22], signifying the role of etiolation in the adventitious root formation of stem cuttings. Etiolation maintains a balance among phytohormones (auxin and cytokinin) in different conditions to aid developmental processes and organogenesis [23]. Etiolation declines the lignification of shoots which results in less development of sclerenchyma tissues. Therefore, the penetration of phytohormones into plants is easy because of less accumulation of cell wall deposits and thin cell walls [24].

The present study focused on identifying the key DEGs with their functions in the process of etiolated hypocotyls in *R. pseudoacacia* during the formation of the adventitious root. We examined the global gene expression of the control and lower segments of etiolated hypocotyl treated with NAA at three time points (60 h, 66 h, and 72 h). The RNA-seq data depicted that *Glycine max* had the greatest number of hits from *R. pseudoacacia* during transcriptome assembly, reflecting the high sequence resemblance.

Based on enriched pathways (metabolic pathway, biosynthesis of secondary metabolites, phenylpropanoid biosynthesis, protein processing in the endoplasmic reticulum, carbon metabolism, starch and sucrose metabolism, and plant hormone transduction) analysis, we identified key functional genes, playing a significant role in adventitious root formation with exogenous NAA.

3.1. Histological Changes for the Process of Adventitious Root Formation in R. pseudoacacia

Generally, three stages were observed during adventitious root formation, including induction, initiation, and elongation [21]. The origin of the dome-shaped primordium was near the vascular cambium and secondary phloem tissues. Root formation is a continuous process and, therefore, cell division, cell elongation, and cell differentiation occur continuously to form root primordia [22] and differentiated adventitious root [23]. In the present study, we observed that the root primordia emerged out from the hypocotyl's outer layer at 72 h of hormone treatment (Figure 1). The histology at 60 h, 66 h, and 72 h showed obvious changes (Figure 1); however, in control conditions, the hypocotyl tissues up to 72 h did not exhibit any growth. At each time point (60 h, 66 h, and 72 h), there was a clear difference between the treatment and control. The small callus was formed on the wounded sites of the hypocotyl, culturing in the medium at 72 h. Anatomical changes also showed that both new and old primordia were present in which the organization and differentiation of cells had started, which contributed to the formation of adventitious roots in poplar "NL895". The results are consistent with previous findings [24,25]. Therefore, it is suggested that there were no clear boundaries between stages.

3.2. Functional Annotation of DEGs and Expression Analysis

RNA-sequencing was performed for understanding the gene expression changes during the formation of adventitious roots in *R. pseudoacacia*. The data depicted that the significant number of DEGs during the early stages of adventitious root formation are not similar with the DNA microarray analysis.

Significantly enriched GO terms for the DEGs in all comparisons included biological processes, including the metabolic process, catalytic activity, and cellular process (Figure 3). According to the KEGG enrichment analysis, pathways associated with metabolic processes and the biosynthesis of secondary metabolites were the most influenced by etiolation. For example, the 40S ribosomal protein S5 A, classified in the ribosome pathway, was expressed only in etiolated tissues. The 40S ribosomal protein S5 A encodes the ribosomal protein S5. Cell division processes were delayed or distributed in a heterozygous *Arabidopsis thaliana* mutant, and development was arrested completely at an early embryonic stage in a homozygous mutant [26]. This indicates that cell division and the development of etiolated tissues may be postponed or restricted.

3.3. Plant Hormone Signal Transduction Pathway

3.3.1. Auxin

In the present study, a significant number of DEGs were expressed in the auxin signaling pathways (AUX/IAA, SAUR, and GH3), cytokinin signaling (*B-ARRs*, *APL*, and *EFM*), abscisic acid signaling (*PP2C*, *SNRK2-7* and *ABI5*), salicylic acid signaling, jasmonic acid, brassinosteroids (*MYC2*, *TCH4*, *BRI1*, *SPL12*, *TGA9*, and *PR-1-LIKE*), and gibberellin. These genes were expressed at various stages of adventitious root formation at 60 h, 66 h, and 72 h. The adventitious root formation produced by wounding in cuttings is dependent on polar auxin transport and the early gathering of IAA in the rooting zone [27]. These results are inconsistent with previous findings reported by Ren, Hu [28] that during adventitious root formation in *R. pseudoacacia* stem cuttings, the most auxin-related genes (*AUX/IAA(IAA19)*, *GH3*, and *SAUR*) were upregulated with exogenous auxin treatment [29]. In addition, the *GH3.3* gene was upregulated during adventitious root formation through hypocotyl tissue culture for hypocotyls of *R. pseudoacacia*, which contradicts with the previous findings in other species [30]. Previously, *SAUR* and *GH3.* The type B cytokinin response regulators greatly influence the number of adventitious roots by increasing or decreasing the expression levels. The type B cytokinin response regulators greatly influence the number of adventitious roots by increasing or decreasing the expression levels were upregulated, and *IAA* was downregulated in etiolated walnut stems [31]. However, in rice, the *OsGH3* gene was upregulated on auxin treatment, and *GH3.3* was positively correlated with the regulation of adventitious root formation [30] The above mentioned genes may play a key role during the adventitious rooting of *R. pseudoacacia.*

3.3.2. Cytokinin

Cytokinin is antagonistic to auxin and mainly acts as a suppressor of adventitious root formation in many species [32]. There are two main types of cytokinin (type A and type B), which positively regulate cytokinin signaling. *A-ARRs* negatively regulate the response of cytokinin and are transcriptionally regulated by *B-ARRs* [33]. We found that genes *B-ARRs* (gene957, gene30838), *APL* (25497), and *EFM* (gene36128) are involved and encode type *B-ARR*, which showed upregulation on three tested time points (60 h, 66 h, 72 h). The relative expressions of cytokinin and two pseudo-response regulators 2(*PRR2*) were observed under the NAA treatment. The expression of *PRR2* (gene957) first de-creased and then increased from BL-60 h to BL-72 h (Figure 6b), while the expression of *PRR2* (gene30838) continuously increased from BL-60 h to BL-72 h (Table S3). The type B cytokinin response regulators greatly influence the number of adventitious roots by increasing or decreasing the expression levels [32,34], whereas *APL* is essential for maintaining phloem cell identity [35]. *AtMYB96* acts as an important molecular link between salicylic acid and abscisic acid crosstalk, through which it can enhance the resistance against pathogens in *Arabidopsis thaliana* [36]. These results indicate that the differential expression of type *B-ARRs* may play a role in *R. pseudoacacia* adventitious root formation induced by auxin. These proposed interactions and the mechanisms underlying them need further experimental proof.

3.3.3. Abscisic Acid

It is well known that abscisic acid acts as a repressor in root initiation and negatively affects adventitious root formation [37]. Our data indicated that under NAA treatment, the differentially expressed genes associated with abscisic acid are *PP2C* (gene22236), *SNRK2-7* (gene4461), and *ABI5* (gene9262). The relative expression of abscisic acid, protein phosphatase 2CA *(PP2C*, gene22236) continuously increased from BL-60 h to BL-72 h under NAA treatment. *ABI5* is a primary leucine zipper transcription factor that functions in the core abscisic acid signaling pathway comprising *PYR/PYL/RCAR* receptors, the negative regulator of *PP2C* phosphatases, and the positive regulator of *SnRK2*, through the regulation of gene expression. Moreover, during partial submergence, the abscisic acid concentration in the petioles of *Rumex palustris* and stems of *S. dulcamara* sharply decreased due to a fast downregulation of abscisic acid biosynthesis and upregulation of

abscisic acid breakdown [38]. In addition, the abscisic acid downstream signaling gene *ABF* is upregulated in Red Fife [39]. Abscisic acid insensitive 5 (*ABI5*, gene9262) expression decreased from BL-60 h to BL-66 h and increased from BL-66 h. Additionally, abscisic acid induces *ABI5* expression in the lateral root tips. These results indicate that *ABI5* acts as a negative regulator of lateral root development in the presence of stress [40], which may play a role during adventitious root formation of *R. pseudoacacia*. These results indicate that differential expression of abscisic acid genes may play a vital role during the adventitious rooting of *R. pseudoacacia*.

3.3.4. Gibberellic Acid

The *BnSCL1* gene is regulated by auxin and is functionally associated with root development [41]. Scarecrow-like genes are induced in rooting-competent cells at the earliest stages of adventitious root formation in the presence of exogenous auxin [42]. In this study, *DELLA*, *scarecrow-like 15* (SCL15) (gene1989) has been found with decreasing expression followed by increasing expression pattern from BL-60 h to BL-72 h. The exogenous application of GA inhibits adventitious root formation in rice, and rice mutants deficient in GA biosynthesis develop more adventitious roots [43]. GA promotes the proteasome-mediated degradation of *DELLA* proteins [44]. Therefore, it is concluded that GA, through *DELLA*, repressed the expression of other genes [45]. Thus, GA-related genes may mediate the interaction of GA and auxin to regulate adventitious root formation.

3.3.5. Jasmonic Acid, Brassinosteroids and Salicylic Acid

Jasmonic acid and brassinosteroids play a crucial role in adventitious root formation. Adventitious roots sometimes form directly from sites in wounded vascular tissues [46]. In the present study, jasmonic acid genes, *MYC2* (gene13924, and gene35754), brassinosteroids genes *TCH4* (xyloglucan endo trans glycosylase 6; gene5477) and *BRI1* (squamosa promoter-binding protein-like 12) (*SPL12*; gene3355), pathogenesis-related gene 1 (*PR1*; gene13913), and *TGA9* (gene24193) were differentially expressed during adventitious root formation. Jasmonic acid has been recently shown to be a negative regulator of adventitious roots that acts downstream of the auxin pathway in *Arabidopsis thaliana*. The relative expressions of brassinosteroid genes, (*SPL12*; gene3355) and (*TCH4*; gene5477), were found (Table S3). Similar to auxin, brassinosteroids promote root growth at low concentrations but inhibit growth at high concentrations [47].

Jasmonic acid is a positive or a negative regulator of adventitious root formation [48]. *MYC2* and *bHLH* are very important for the entire jasmonic acid signaling pathway [49], and help in the regulation of root growth and development, cellular proliferation, and differentiation [50]. The expression of *TCH4* is upregulated by darkness, increased auxin, and brassinosteroids [51]. The expression of the *TCH4-GUS* reporter gene in transgenic *Arabidopsis thaliana* is significantly higher in growing parts, such as the elongating hypocotyls of seedlings grown under low light intensity, auxin and brassinosteroids. Increased *TCH4* expression may be an important step in hormone-induced alterations for cell expansion [52]. Moreover, the expressions of *SPL* genes may be regulated by light and phytohormones [53]. *SPLs* are also involved in the appropriate timing of the root developmental process [54]. The relative expression of salicylic acid, motif-binding protein 9 (*TGA9*) (gene24193) expression continuously decreased from BL-60 h to BL-72 h (Table S3). Salicylic acid production, which usually occurs as a response to various stresses, has also been reported to trigger plant root development. *PR1* (gene13913) and *TGA9* (gene24193) are important genes in salicylic acid signaling. The present findings suggested that genes involved in auxin, abscisic acid, brassinosteroid, jasmonic acid, cytokinin, gibberellin, and salicylic acid signaling may interact with auxin to mediate adventitious root formation. However, the interaction of hormones with auxin during adventitious root formation in *R. pseudoacacia* is not clear.

3.3.6. Starch and Sucrose Metabolism Pathway

Auxins help in the mobilization and hydrolysis of starch and sugars to the cutting base [55]. The DEGs encoded by the starch and sucrose metabolism include *SUS3* (sucrose synthase 3), *AIR3* (auxin-induced in root cultures 3), *ADG2* (ADP glucose pyro phosphorylase 2), plant invertase/pectin methyl esterase inhibitor superfamily, *PMEI9*, *PMEI3* (pectin methylesterase inhibitor 19, 13) and *BMY5*, *BAM6* (beta-amylase 5, beta-amylase 6). In the present study, the relative expression level of *SUS3* (gene9499) slightly increased from BL-60 h to BL-72 h (Figure 7b). β-Amylase helps in the degradation of starch [55], maltose, sucrose, and cell wall components, but decreases starch content [56], which means etiolation requires more energy as compared to the control. In addition, *SUS*s, as a biocatalyst, encode sucrose synthase and improve adventitious root formation during lateral stages [57]. Additionally, *AIR3* encodes subtilisin-like proteases [58] that help to facilitate easy root emergence by weakening the connection among cells in *Arabidopsis thaliana* during root development [59]. In contrast, *AIR3* (gene30616) expression continuously decreased from BL-60 h to BL-72 h (Figure 7b). Three genes of the plant invertase/pectin methyl esterase inhibitor superfamily were found. The DEGs were upregulated in the starch and sucrose metabolism pathway [60]. Moreover, glucose pyro-phosphorylase is a key metabolite and precursor of carbohydrate formation [61]. It plays a role in the formation of the pericycle during starch/sucrose production, which can be used to fine-tune roots in Arabidopsis by the accessibility of carbon sources [62]. Our study shows that adventitious root formation and elongated etiolated seedlings may require more sucrose as an energy source. These expression changes and results concluded that the mechanism in which etiolation promotes adventitious root formation might be linked with more energy supply, hormone synthesis, or different signaling pathways.

3.3.7. Phenylpropanoid Biosynthesis Pathway

The phenylpropanoids and related flavonoids of the phenylpropanoid metabolism pathway might play their role in NAA-induced adventitious root formation. Phenylpropanoids convert phenylalanine to an activated cinnamic acid derivative, which leads to the production of flavonoids or iso-flavonoids [63]. Among phenylpropanoid DEGs, *Arabidopsis thaliana peroxidase CB* (gene5) expression increased continuously from BL-60 h to BL-72 h (Figure 8b). In addition, peroxidase superfamily protein (gene12931) (Figure 8b) and peroxidase 2 (gene12930) showed a similar trend, first increasing from BL-60 h to BL-66 h and then decreasing from BL-66 h to BL-72 h (Table S3). The phenylpropanoids from the secondary metabolic pathway play an important role in auxin-induced adventitious rooting [64]. Phenolic acids and flavonoids from the phenylpropanoid pathway [65] majorly contribute to cell division and differentiation [66] during in vitro rooting [67]. Therefore, prior changes in phenylpropanoids contribute to *Arabidopsis thaliana* root development. In this study, the expression of *peroxidase 40* (gene22473) (Figure 8b) and telomeric DNA-binding protein 2 (gene22265) increased continuously from BL-60 h to BL-72 h (Table S3). Moreover, specific peroxidases help to maintain the cell division and the differentiation in root meristematic cells [68] during root emergence [69]. In stem cuttings, plant growth, differentiation, and development are controlled by total peroxidase activity [70]. Moreover, peroxidases may promote cell elongation by producing more free radicals that may loosen the cell wall [71], which helps in the penetration of phytohormones for the formation of adventitious roots. Therefore, DEGs involved in the phenylpropanoid pathway, which may have a key role in adventitious root formation in *R. pseudoacacia*.

3.3.8. Carbon Metabolism Pathway

Carbon metabolism shares sucrose metabolites, which are converted to hexose by *SUS* and INV (invertase) for the root primordium and root elongation [72]. *PSAT1* promotes cell proliferation and chemoresistance in vitro [73]. Therefore, the phosphorylated route for serine synthesis is reportedly associated with meristematic or rapidly proliferating plant tissues [72]. In this study, DEGs in carbon metabolism might be playing a plausible

role during adventitious root formation. These genes included *PSAT1* (phosphoserine aminotransferase 1), *SERAT3;2* (serine acetyltransferase 3;2), *GOX1* (glycolate oxidase 1), *FBA1* (fructose-bisphosphate aldolase 1), *PFK7* (phosphofructokinase 7), *PRK* (phosphoribulokinase) and *SHM1* (serine hydroxy methyltransferase 1). Moreover, *SERAT3;2* has low substrate affinities and low gene expression levels [74] but plays roles in later developmental stages of root formation and metabolism [75]. In addition, fructose-bisphosphate aldolase catalyzes an aldol cleavage of fructose-1,6- bisphosphate to dihydroxyacetone-phosphate [76], which plays a significant role in regulating signal transduction [77]. It has been reported that fructose-bisphosphate aldolase (*FBA*) plays an important physiological role in accelerating cell elongation to promote root elongation in rice [72]. The seed germination and root elongation of *AtFBA1* knock-out plants exhibited sensitivity to abscisic acid, indicating that *AtFBA1* expression and aldolase activity are important for changing abscisic acid expression in plants [78]. Under NAA treatment, the relative expression level of *GOX1* (gene25254), *FBA1* (gene16722), and *PFK7* (gene23954) first decreased at BL-60 h to BL-66 h, followed by an increase from stage BL-66 h to BL-72 h, and the highest expression of the first two genes was observed at BL-72 h and for the last one at BL-60 h, respectively (Figure 9b). Phosphofructokinase (*PFK*) is an important enzyme in central carbon metabolism that promotes carbon flux into the glycolytic pathway [79]. *PFK* was upregulated only in JM-262. In addition, when plants were grown under nitrogen-free conditions, the genes involved in nitrogen compound metabolism, carbon metabolism, amino acid metabolism, and photosynthesis were downregulated in roots and leaves [80]. Besides, only three genes (*GOX1*, *GOX2*, and *GOX3*) out of five from *Arabidopsis* were expressed in the elongation zone. *GOX1* and *GOX2* are the major glycolate oxidase enzymes [81], which catalyze the oxidation of glycolate to glyoxylate [82]. Therefore, the expression suggests that these *GOX* family members are associated with distinct functions in roots [81]. All the DEGs in carbon metabolism may play a role during adventitious root formation.

4. Materials and Methods

4.1. Plant Material

R. pseudoacacia-148 is a half-sib, and their seeds were selected based on national improved variety, from Qingshui County, Gansu Province, China. To investigate the kinetics of adventitious root formation, preparation of RNA extraction for high-throughput sequencing was performed, using tissue culture plantlets of *R. pseudoacacia*-148 as plant material. Sterilized seeds were germinated on Murashige and Skoog medium without hormones. Dark and light treatments were performed according to Masomi et al. [83], with a little modification—the hypocotyl was sliced from the primary root and hypocotyl junction, but also hypocotyls were wounded for easy uptake of hormones. Seeds were given pretreatment of darkness for 4 days continuously followed by 4 days' photoperiod 16/8 h, and controlled samples were kept under 16/8 h photoperiod for 8 days. After completing 8 days, the 1 cm lower part of elongated (treated) and non-elongated (control) hypocotyls was sliced from the lower portion of the seedlings. These parts of treated and control were evaluated for adventitious root response by growing into Murashige and Skoog medium containing hormone (NAA 0.3 mg/L) under 16/8 h photoperiod. Samples for RNA-sequencing were collected at 60 h, 66 h, and 72 h from control and treated samples. Dark pretreated samples were given the names BL-60 h, BL-66 h, and BL-72 h, while control samples were given the names BL-CK60 h, BL-CK66 h, and BL-CK72 h.

4.2. Anatomical and Microscopic Analysis

For histological analysis, the same method and growth condition as RNA-Seq were employed for collecting the 1 cm lower portion of the hypocotyl. At least 20 hypocotyls were collected for each time point with three biological replicates. The collected tissues were fixed in formaldehyde acetic acid FAA (50% ethanol, 38% formaldehyde, acetic acid 5 mL/100 mL, and glycerol 5 mL/100 mL) and then treated with the protocol as described by [84]. A lower portion of the hypocotyl (8 µm) was prepared with a rotary microtome

(LEICA RM2235) for histological study and then stained with safranin (1%) and fast-green (0.5%). All sections were examined and photographed with LEICA DMI40008 microscope for different tested time points.

4.3. RNA Extraction, Deep Sequencing, Functional Annotation, Pathway Enrichment, and qRT-PCR Analysis

Total RNA was extracted from all 12 samples (control and treatment), and RIN value (28S/18S) and RNA purity (OD260/280) were detected using ultraviolet spectrophotometer Nanodrop. The first-strand cDNAs were synthesized by using the Takara Reverse Transcription System (TaKaRa, Tokyo, Japan). The specific PCR primers for the selected candidate gene were designed and primer sequences are listed in Table S4. The qRT-PCR reactions were performed in a Mini Opticon Real-Time PCR System (Bio-Rad, Hercules, CA, USA). SYBR Green Master Mix Reagent (TaKaRa, Shuzo, Otsu, Tokyo, Japan) was used per protocol. The comparative 2-ΔΔCTmethod was used to calculate the relative expression levels [47]. The heat map for the gene expression profiles was generated with Mev 4.0 software (http://www.tm4.org/) [48]. Actin was used as a housekeeping gene.

Constructed libraries were tested using the Agilent 2100 bioanalyzer and concentration was quantified using the ABI Step One Plus real-time PCR system. After quality inspection, sequencing was performed by Illumina Hi-Seq sequencer. Raw image data obtained by high-throughput Illumina Hi-Seq-2500 were converted to sequences by CASAVA bas call analysis and stored in FASTQ file format, which contained sequence information. The sequencing data and mapping results are shown in Table 1. All samples of treatment and control were grouped. We selected three time points (60 h, 66 h, and 72 h) based on histological results. Samples' names were given on the basis of the common name of *R. pseudoacacia*, Black Locust (BL), at all time points. The treatment itself had three comparisons and three comparisons between control and treatment at three time points (60 h, 66 h, and 72 h). Treatment groups (comparisons) at three time points were BL-60 h vs. BL-66 h, BL-60 h vs. BL-72 h, BL-66 h vs. BL-72 h, and control and treatment groups (comparisons) were BL-CK60 h vs. BL-60 h, BL-CK60 h vs. BL-66 h, BL-CK60 h vs. BL-72 h. After getting clean reads, we used HISAT (D, 2015) to compare clean reads to the reference (*R. pseudoacacia*) genome. HISAT is developed by John Hopkins University and it aligns very quickly [85]. HISAT combined with String-Tie [86] gives more accurate gene reconstruction and better prediction of expression level than programs like cufflinks. DEG analysis was performed with DESeq2 = (Fold Change) ≥ 2 with adjusted value ≤ 0.05 and RSEM (v1.2.12) to calculate the expression levels of genes and transcripts (http://deweylab.biostat.wisc.edu/rsem). For functional annotation, the data were searched against the NR (http://www.ncbi.nlm.nih.gov/), Kyoto Encyclopedia of Genes and Genomes (KEGG) (http://www.genome.jp/kegg/) and GO (http://www.ncbi.nlm.nih.gov/COG/) databases with a typical cut-off value of E-value $< 1 \times 10^{-5}$. Blast2GO v2.5 (E-value $< 1 \times 10^{-6}$) software was used to assign Gene Ontology (GO) annotations. After the GO and KEGG annotation, enrichment analysis was carried out using the Phyper function in R software. The *p*-values and functional divergence ratio (FDR) were evaluated by considering an FDR ≤ 0.01 value as significant enrichment.

5. Conclusions

The present study describes the important histological events of early root formation and biological pathways occurring during adventitious root formation in *R. pseudoacacia*-148 under etiolation as a pretreatment. The histological analysis provided the origin and timing of different stages of adventitious root formation. Etiolation increased the number and length of adventitious roots and promoted root formation earlier than the control at 72 h after 8 days of pretreatment. The present study provides novel information for understanding the relationship and involvement of candidate genes (*AUX/IAA*, *SAUR*, *GH3.3*, *PRR2*, *SCL15*, *MYC2*, *SUS3*, *AIR3*, and *SHM1*) in the various important pathways (plant hormone signal pathway, starch and sucrose metabolism, phenylpropanoids, carbon metabolism) that regulate adventitious root formation. The current study provides an

overview of the transcriptomic changes that occur during adventitious root formation in *R. pseudoacacia*. Based on annotation and enrichment analysis, the response of *R. pseudoacacia* during adventitious root formation has been demonstrated. This information will be helpful for future studies on how etiolation responds during the formation of adventitious roots in *R. pseudoacacia* and other woody species. The whole-genome sequence of *R. pseudoacacia* has not yet been released; our study will provide reference data for molecular research. However, many details of the molecular mechanism by which etiolation promotes adventitious root formation in *R. pseudoacacia* remain unclear. These will be our research focus in future studies. Adventitious root formation is a complex biological process regulated by different pathways. Our work provides a transcriptomic overview of NAA-induced adventitious root formation. However, owing to technical limitations, our study did not offer any post-transcriptional or (post)-translational evidence for adventitious root formation, which is also an important regulatory pathway for adventitious root formation. Whether these pathways are also involved in NAA-induced adventitious root formation still needs further analysis.

Supplementary Materials: The following are available online at https://www.mdpi.com/article/10.3390/f12060789/s1, Figure S1: The distribution interval of gene expression in RNA-Seq data of each sample, Figure S2: Correlation and principal component analysis, Figure S3: Gene ontology classification of DEGs among control and treatment and among treatment three time points, Table S1: Gene ontology classification of different comparisons, Table S2: Kyoto Encyclopedia of Genes and Genomes (KEGG) of different comparisons, Table S3: DEGs identified in different pathways at three time points with respective control (CK60, 60h, 66h, 72h) with expression values in log2(FPKM), Table S4: Sequence of primers used in the qRT-PCR analysis to validate gene expression.

Author Contributions: Conceptualization, Y.L., M.Z.M. and S.U.D.; methodology, Y.L., M.Z.M. and S.U.D.; software, M.I.; validation, Z.Z., C.H. and Y.S.; formal analysis, T.P., Z.U.N., M.Z.M., S.U.D., Y.L. and M.I.; data curation, M.I., M.Z.M., S.U.D. and T.P.; writing—original draft preparation, M.Z.M. and S.U.D.; writing—review and editing, M.Z.M., S.U.D., M.A.M. and A.B.; visualization, Y.S.; supervision, Y.L.; project administration, Y.L.; funding acquisition, Y.L. All authors have read and agreed to the published version of the manuscript.

Funding: This research was funded by the National Natural Science Foundation of China (31570677) and the National Key R&D Program of China (2017YFD0600503).

Institutional Review Board Statement: Not applicable.

Informed Consent Statement: Not applicable.

Data Availability Statement: Not applicable.

Conflicts of Interest: The authors declare no conflict of interest.

References

1. Zhang, Z.; Sun, Y.; Han, C.; Dong, L.; Guo, Q.; Li, X.; Li, Y. *Integrated Analysis of the Physiology, RNA, and microRNA Involved in Black Locust (Robinia pseudoacacia) Rejuvenation*. 2019. Available online: http://doi.org/10.21203/rs.2.10375/v1 (accessed on 16 March 2021).
2. Rédei, K. *Black Locust (Robinia pseudoacacia L.) Growing in Hungary*; Publications of the Hungarian Forest Research Institute: Budapest, Ungarn, 1998.
3. Rédei, K.; Keserű, Z.; Csiha, I.; Rásó, J.; Bakti, B.; Takács, M. Improvement of black locust (*Robinia pseudoacacia* L.) growing under marginal site conditions in Hungary: Case studies. *Acta Agrar. Debr.* **2018**, *74*, 129–133. [CrossRef]
4. Ragonezi, C.; Klimaszewska, K.; Castro, M.R.; Lima, M.; de Oliveira, P.; Zavattieri, M.A. Adventitious rooting of conifers: Influence of physical and chemical factors. *Trees* **2010**, *24*, 975–992. [CrossRef]
5. Meng, B.N.; Peng, Z.D.; Zhang, Z.L.; Xu, H.M.; Li, Y. Research on cuttage of tetraploid black locust (*Robinia pseudoacacia* L.) hardwood treated by low temperature sand storage and plant growth regulator. *Heilongjiang Agric. Sc.* **2010**, *8*, 85–88.
6. Da Costa, C.T.; De Almeida, M.R.; Ruedell, C.M.; Schwambach, J.; Maraschin, F.D.S.; Fett-Neto, A.G. When stress and development go hand in hand: Main hormonal controls of adventitious rooting in cuttings. *Front. Plant Sci.* **2013**, *4*, 133. [CrossRef]
7. Bellini, C.; Pacurar, D.I.; Perrone, I. Adventitious roots and lateral roots: Similarities and differences. *Annu. Rev. Plant Biol.* **2014**, *65*, 639–666. [CrossRef]

8. Lu, N.; Dai, L.; Luo, Z.; Wang, S.; Wen, Y.; Duan, H.; Li, Y. Characterization of the transcriptome and gene expression of tetraploid black locust cuttings in response to etiolation. *Genes* **2017**, *8*, 345. [CrossRef]
9. Klopotek, Y.; Haensch, K.T.; Hause, B.; Hajirezaei, M.R.; Druege, U. Dark exposure of petunia cuttings strongly improves adventitious root formation and enhances carbohydrate availability during rooting in the light. *J. Plant Physiol.* **2010**, *167*, 547–554. [CrossRef] [PubMed]
10. Lakehal, A.; Bellini, C. Control of adventitious root formation: Insights into synergistic and antagonistic hormonal interactions. *Physiol. Plant.* **2019**, *165*, 90–100. [CrossRef]
11. De Klerk, G.-J.; Guan, H.; Huisman, P.; Marinova, S. Effects of phenolic compounds on adventitious root formation and oxidative decarboxylation of applied indoleacetic acid in Malus 'Jork 9'. *Plant Growth Regul.* **2011**, *63*, 175–185. [CrossRef]
12. Kevers, C.; Hausman, J.F.; Faivre-Rampant, O.; Dommes, J.; Gaspar, T. *What We Have Learned about the Physiology of In Vitro Adventitious Rooting of Woody Plants and How It Relates to Improvements in the Practice*; Research Signpost: Kerala, India, 2009; pp. 209–225.
13. Zaman, M.; Kurepin, L.V.; Catto, W.; Pharis, R.P. Evaluating the use of plant hormones and biostimulators in forage pastures to enhance shoot dry biomass production by perennial ryegrass (*Lolium perenne* L.). *J. Sci. Food Agric.* **2016**, *96*, 715–726. [CrossRef]
14. Richards, M.R.; Rupp, L.A. Etiolation improves rooting of bigtooth maple cuttings. *HortTechnology* **2012**, *22*, 305–310. [CrossRef]
15. Batten, D.; Mullins, M. Ethylene and adventitious root formation in hypocotyl segments of etiolated mung-bean (*Vigna radiata* (L.) Wilczek) seedlings. *Planta* **1978**, *138*, 193–197. [CrossRef] [PubMed]
16. Pacurar, D.I.; Perrone, I.; Bellini, C. Auxin is a central player in the hormone cross-talks that control adventitious rooting. *Physiol. Plant.* **2014**, *151*, 83–96. [CrossRef] [PubMed]
17. De Klerk, G.-J.; Van Der Krieken, W.; de Jong, J.C. Review the formation of adventitious roots: New concepts, new possibilities. *Vitr. Cell. Dev. Biol. Plant* **1999**, *35*, 189–199. [CrossRef]
18. Legué, V.; Rigal, A.; Bhalerao, R.P. Adventitious root formation in tree species: Involvement of transcription factors. *Physiol. Plant.* **2014**, *151*, 192–198. [CrossRef]
19. Olatunji, D.; Geelen, D.; Verstraeten, I. Control of endogenous auxin levels in plant root development. *Int. J. Mol. Sci.* **2017**, *18*, 2587. [CrossRef]
20. Wiesman, Z.; Lavee, S. Enhancement of IBA stimulatory effect on rooting of olive cultivar stem cuttings. *Sci. Hortic.* **1995**, *62*, 189–198. [CrossRef]
21. Li, S.-W.; Xue, L.; Xu, S.; Feng, H.; An, L. Hydrogen peroxide acts as a signal molecule in the adventitious root formation of mung bean seedlings. *Environ. Exp. Bot.* **2009**, *65*, 63–71. [CrossRef]
22. Koyuncu, F.; Balta, F. Adventitious root formation in leaf-bud cuttings of tea (*Camellia sinensis* L.). *Pak. J. Bot.* **2004**, *36*, 763–768.
23. Goldfarb, B.; Hackett, W.P.; Furnier, G.R.; Mohn, C.A.; Plietzsch, A. Adventitious root initiation in hypocotyl and epicotyl cuttings of eastern white pine (*Pinus strobus*) seedlings. *Physiol. Plant.* **1998**, *102*, 513–522. [CrossRef]
24. Smith, N.; Wareing, P. The distribution of latent root primordia in stems of Populus× robusta, and factors affecting the emergence of preformed roots from cuttings. *For. Int. J. For. Res.* **1972**, *45*, 197–209. [CrossRef]
25. Carlson, M.C. Nodal adventitious roots in willow stems of different ages. *Am. J. Bot.* **1950**, *37*, 555–561. [CrossRef]
26. Weijers, D.; Franke-van Dijk, M.; Vencken, R.J.; Quint, A.; Hooykaas, P.; Offringa, R. An Arabidopsis Minute-like phenotype caused by a semi-dominant mutation in a RIBOSOMAL PROTEIN S5 gene. *Development* **2001**, *128*, 4289–4299. [CrossRef] [PubMed]
27. Garrido, G.; Ramón Guerrero, J.; Angel Cano, E.; Acosta, M.; Sánchez-Bravo, J. Origin and basipetal transport of the IAA responsible for rooting of carnation cuttings. *Physiol. Plant.* **2002**, *114*, 303–312. [CrossRef]
28. Ren, H.; Hu, H.; Luo, X.; Zhang, C.; Li, X.; Li, P.; Shen, C. Dynamic changes of phytohormone signaling in the base of Taxus media stem cuttings during adventitious root formation. *Sci. Hortic.* **2019**, *246*, 338–346. [CrossRef]
29. Dumas, E.; Monteuuis, O. In vitro rooting of micropropagated shoots from juvenile and mature Pinus pinaster explants: Influence of activated charcoal. *Plant Cell Tissue Organ Cult.* **1995**, *40*, 231–235. [CrossRef]
30. Yang, G.; Chen, S.; Wang, S.; Liu, G.; Li, H.; Huang, H.; Jiang, J. BpGH3. 5, an early auxin-response gene, regulates root elongation in Betula platyphylla× Betula pendula. *Plant Cell Tissue Organ Cult.* **2015**, *120*, 239–250. [CrossRef]
31. Keuskamp, D.H.; Pollmann, S.; Voesenek, L.A.; Peeters, A.J.; Pierik, R. Auxin transport through PIN-FORMED 3 (PIN3) controls shade avoidance and fitness during competition. *Proc. Natl. Acad. Sci. USA* **2010**, *107*, 22740–22744. [CrossRef]
32. Ramírez-Carvajal, G.A.; Morse, A.M.; Dervinis, C.; Davis, J.M. The cytokinin type-B response regulator PtRR13 is a negative regulator of adventitious root development in Populus. *Plant Physiol.* **2009**, *150*, 759–771. [CrossRef] [PubMed]
33. Naseem, M.; Kaltdorf, M.; Dandekar, T. The nexus between growth and defence signalling: Auxin and cytokinin modulate plant immune response pathways. *J. Exp. Bot.* **2015**, *66*, 4885–4896. [CrossRef] [PubMed]
34. Gonzalez-Rizzo, S.; Crespi, M.; Frugier, F. The Medicago truncatula CRE1 cytokinin receptor regulates lateral root development and early symbiotic interaction with Sinorhizobium meliloti. *Plant Cell* **2006**, *18*, 2680–2693. [CrossRef]
35. Bonke, M.; Thitamadee, S.; Mähönen, A.P.; Hauser, M.T.; Helariutta, Y. APL regulates vascular tissue identity in Arabidopsis. *Nature* **2003**, *426*, 181–186. [CrossRef]
36. Prabu, G.; Prasad, D.T. Functional characterization of sugarcane MYB transcription factor gene promoter (PScMYBAS1) in response to abiotic stresses and hormones. *Plant Cell Rep.* **2012**, *31*, 661–669. [CrossRef]
37. De Smet, I.; Zhang, H.; Inze, D.; Beeckman, T. A novel role for abscisic acid emerges from underground. *Trends Plant Sci.* **2006**, *11*, 434–439. [CrossRef]

38. Dawood, T.; Yang, X.; Visser, E.J.; Te Beek, T.A.; Kensche, P.R.; Cristescu, S.M.; Rieu, I. A co-opted hormonal cascade activates dormant adventitious root primordia upon flooding in Solanum dulcamara. *Plant Physiol.* **2016**, *170*, 2351–2364. [CrossRef]
39. Goessen, R. *Exploring the Involvement of Gene Regulatory Variation in Wheat Improvement with Network Analysis*. 2018. Available online: https://edepot.wur.nl/433739 (accessed on 16 March 2021).
40. Shkolnik-Inbar, D.; Bar-Zvi, D. ABI4 mediates abscisic acid and cytokinin inhibition of lateral root formation by reducing polar auxin transport in Arabidopsis. *Plant Cell* **2010**, *22*, 3560–3573. [CrossRef]
41. Gao, M.-J.; Parkin, I.; Lydiate, D.; Hannoufa, A. An auxin-responsive SCARECROW-like transcriptional activator interacts with histone deacetylase. *Plant Mol. Biol.* **2004**, *55*, 417–431. [CrossRef]
42. Vielba, J.M.; Díaz-Sala, C.; Ferro, E.; Rico, S.; Lamprecht, M.; Abarca, D.; Sánchez, C. CsSCL1 is differentially regulated upon maturation in chestnut microshoots and is specifically expressed in rooting-competent cells. *Tree Physiol.* **2011**, *31*, 1152–1160. [CrossRef] [PubMed]
43. Lo, S.-F.; Yang, S.Y.; Chen, K.T.; Hsing, Y.I.; Zeevaart, J.A.; Chen, L.J.; Yu, S.M. A novel class of gibberellin 2-oxidases control semidwarfism, tillering, and root development in rice. *Plant Cell* **2008**, *20*, 2603–2618. [CrossRef] [PubMed]
44. Steffens, B.; Sauter, M. Epidermal cell death in rice is regulated by ethylene, gibberellin, and abscisic acid. *Plant Physiol.* **2005**, *139*, 713–721. [CrossRef] [PubMed]
45. Li, K.; Liang, Y.; Xing, L.; Mao, J.; Liu, Z.; Dong, F.; Zhang, D. Transcriptome analysis reveals multiple hormones, wounding and sugar signaling pathways mediate adventitious root formation in apple rootstock. *Int. J. Mol. Sci.* **2018**, *19*, 2201. [CrossRef]
46. Agulló-Antón, M.Á.; Ferrández-Ayela, A.; Fernández-García, N.; Nicolás, C.; Albacete, A.; Pérez-Alfocea, F.; Acosta, M. Early steps of adventitious rooting: Morphology, hormonal profiling and carbohydrate turnover in carnation stem cuttings. *Physiol. Plant.* **2014**, *150*, 446–462. [CrossRef] [PubMed]
47. Gutierrez, L.; Mongelard, G.; Floková, K.; Păcurar, D.I.; Novák, O.; Staswick, P.; Bellini, C. Auxin controls Arabidopsis adventitious root initiation by regulating jasmonic acid homeostasis. *Plant Cell* **2012**, *24*, 2515–2527. [CrossRef]
48. Lischweski, S.; Muchow, A.; Guthörl, D.; Hause, B. Jasmonates act positively in adventitious root formation in petunia cuttings. *BMC Plant Biol.* **2015**, *15*, 229. [CrossRef]
49. Kazan, K.; Manners, J.M. MYC2: The master in action. *Mol. Plant* **2013**, *6*, 686–703. [CrossRef] [PubMed]
50. Wang, B.-T.; Yu, X.Y.; Zhu, Y.J.; Zhuang, M.; Zhang, Z.M.; Jin, L.; Jin, F.J. Research progress on the basic helix-loop-helix transcription factors of Aspergillus species. *Adv. Appl. Microbiol.* **2019**, *109*, 31–59. [PubMed]
51. Xu, W.; Campbell, P.; Vargheese, A.K.; Braam, J. The Arabidopsis XET-related gene family: Environmental and hormonal regulation of expression. *Plant J.* **1996**, *9*, 879–889. [CrossRef] [PubMed]
52. Xu, W.; Purugganan, M.M.; Polisensky, D.H.; Antosiewicz, D.M.; Fry, S.C.; Braam, J. Arabidopsis TCH4, regulated by hormones and the environment, encodes a xyloglucan endotransglycosylase. *Plant Cell* **1995**, *7*, 1555–1567. [PubMed]
53. Cai, C.; Guo, W.; Zhang, B. Genome-wide identification and characterization of SPL transcription factor family and their evolution and expression profiling analysis in cotton. *Sci. Rep.* **2018**, *8*, 762.
54. Yu, N.; Niu, Q.W.; Ng, K.H.; Chua, N.H. The role of miR156/SPL s modules in Arabidopsis lateral root development. *Plant J.* **2015**, *83*, 673–685. [CrossRef]
55. OuYang, F.; Wang, J.; Li, Y. Effects of cutting size and exogenous hormone treatment on rooting of shoot cuttings in Norway spruce [*Picea abies* (L.) Karst.]. *New For.* **2015**, *46*, 91–105. [CrossRef]
56. Niu, S.; Li, Z.; Yuan, H.; Fang, P.; Chen, X.; Li, W. Proper gibberellin localization in vascular tissue is required to regulate adventitious root development in tobacco. *J. Exp. Bot.* **2013**, *64*, 3411–3424. [CrossRef] [PubMed]
57. Ruedell, C.M.; de Almeida, M.R.; Fett-Neto, A.G. Concerted transcription of auxin and carbohydrate homeostasis-related genes underlies improved adventitious rooting of microcuttings derived from far-red treated Eucalyptus globulus Labill mother plants. *Plant Physiol. Biochem.* **2015**, *97*, 11–19. [CrossRef] [PubMed]
58. Neuteboom, L.W.; Veth-Tello, L.M.; Clijdesdale, O.R.; Hooykaas, P.J.; van der Zaal, B.J. A novel subtilisin-like protease gene from Arabidopsis thaliana is expressed at sites of lateral root emergence. *DNA Res.* **1999**, *6*, 13–19. [CrossRef] [PubMed]
59. Xie, Q.; Frugis, G.; Colgan, D.; Chua, N.H. Arabidopsis NAC1 transduces auxin signal downstream of TIR1 to promote lateral root development. *Genes Dev.* **2000**, *14*, 3024–3036. [CrossRef] [PubMed]
60. Li, S.-W.; Shi, R.F.; Leng, Y.; Zhou, Y. Transcriptomic analysis reveals the gene expression profile that specifically responds to IBA during adventitious rooting in mung bean seedlings. *BMC Genom.* **2016**, *17*, 1–23. [CrossRef] [PubMed]
61. Wakabayashi, K.; Sakurai, N.; Kuraishi, S. Effects of abscisic acid on the synthesis of cell-wall polysaccharides in segments of etiolated squash hypocotyl II. Levels of UDP-neutral sugars. *Plant Cell Physiol.* **1991**, *32*, 427–432. [CrossRef]
62. Ciereszko, I.; Johansson, H.; Kleczkowski, L.A. Interactive effects of phosphate deficiency, sucrose and light/dark conditions on gene expression of UDP-glucose pyrophosphorylase in Arabidopsis. *J. Plant Physiol.* **2005**, *162*, 343–353. [CrossRef]
63. Abu-Abied, M.; Szwerdszarf, D.; Mordehaev, I.; Levy, A.; Belausov, E.; Yaniv, Y.; Sadot, E. Microarray analysis revealed upregulation of nitrate reductase in juvenile cuttings of Eucalyptus grandis, which correlated with increased nitric oxide production and adventitious root formation. *Plant J.* **2012**, *71*, 787–799. [CrossRef]
64. Wei, K.; Wang, L.Y.; Wu, L.Y.; Zhang, C.C.; Li, H.L.; Tan, L.Q.; Cheng, H. Transcriptome analysis of indole-3-butyric acid-induced adventitious root formation in nodal cuttings of *Camellia sinensis* (L.). *PLoS ONE* **2014**, *9*, e107201. [CrossRef]
65. Boudet, A.; Lapierre, C.; Grima-Pettenati, J. Tansley review No. 80. Biochemistry and molecular biology of lignification. *New Phytol.* **1995**, *129*, 203–236. [CrossRef]

66. Tamagnone, L.; Merida, A.; Stacey, N.; Plaskitt, K.; Parr, A.; Chang, C.F.; Martin, C. Inhibition of phenolic acid metabolism results in precocious cell death and altered cell morphology in leaves of transgenic tobacco plants. *Plant Cell* **1998**, *10*, 1801–1816. [CrossRef]
67. Macedo, E.S.; Sircar, D.; Cardoso, H.G.; Peixe, A.; Arnholdt-Schmitt, B. Involvement of alternative oxidase (AOX) in adventitious rooting of Olea europaea L. microshoots is linked to adaptive phenylpropanoid and lignin metabolism. *Plant Cell Rep.* **2012**, *31*, 1581–1590. [CrossRef]
68. Tsukagoshi, H.; Busch, W.; Benfey, P.N. Transcriptional regulation of ROS controls transition from proliferation to differentiation in the root. *Cell* **2010**, *143*, 606–616. [CrossRef] [PubMed]
69. Manzano, C.; Pallero-Baena, M.; Casimiro, I.; De Rybel, B.; Orman-Ligeza, B.; Van Isterdael, G.; Del Pozo, J.C. The emerging role of reactive oxygen species signaling during lateral root development. *Plant Physiol.* **2014**, *165*, 1105–1119. [CrossRef] [PubMed]
70. Cheniany, M.; Ebrahimzadeh, H.; Masoudi-nejad, A.; Vahdati, K.; Leslie, C. Effect of endogenous phenols and some antioxidant enzyme activities on rooting of Persian walnut (*Juglans regia* L.). *Afr. J. Plant Sci.* **2010**, *4*, 479–487.
71. Schopfer, P. Hydroxyl radical-induced cell-wall loosening in vitro and in vivo: Implications for the control of elongation growth. *Plant J.* **2001**, *28*, 679–688. [CrossRef]
72. Ogawa, A.; Ando, F.; Toyofuku, K.; Kawashima, C. Sucrose metabolism for the development of seminal root in maize seedlings. *Plant Prod. Sci.* **2009**, *12*, 9–16. [CrossRef]
73. Vié, N.; Copois, V.; Bascoul-Mollevi, C.; Denis, V.; Bec, N.; Robert, B.; Gongora, C. Overexpression of phosphoserine aminotransferase PSAT1 stimulates cell growth and increases chemoresistance of colon cancer cells. *Mol. Cancer* **2008**, *7*, 14. [CrossRef]
74. Kawashima, C.G.; Berkowitz, O.; Hell, R.; Noji, M.; Saito, K. Characterization and expression analysis of a serine acetyltransferase gene family involved in a key step of the sulfur assimilation pathway in Arabidopsis. *Plant Physiol.* **2005**, *137*, 220–230. [CrossRef] [PubMed]
75. Watanabe, M.; Mochida, K.; Kato, T.; Tabata, S.; Yoshimoto, N.; Noji, M.; Saito, K. Comparative genomics and reverse genetics analysis reveal indispensable functions of the serine acetyltransferase gene family in Arabidopsis. *Plant Cell* **2008**, *20*, 2484–2496. [CrossRef]
76. Rutter, W.J. *Evolution of Aldolase; In Fed. Proceedings*; November–December 1964; Volume 23, pp. 1248–1257. Available online: https://pubmed.ncbi.nlm.nih.gov/14236133/ (accessed on 16 March 2021).
77. Cho, Y.-H.; Yoo, S.-D. Signaling role of fructose mediated by FINS1/FBP in Arabidopsis thaliana. *PLoS Genet* **2011**, *7*, e1001263. [CrossRef]
78. Moon, S.-J.; Shin, D.J.; Kim, B.G.; Byun, M.O. Putative fructose-1, 6-bisphosphate aldolase 1 (AtFBA1) affects stress tolerance in yeast and Arabidopsis. *J. Plant Biotechnol.* **2012**, *39*, 106–113. [CrossRef]
79. Webb, B.A.; Dosey, A.M.; Wittmann, T.; Kollman, J.M.; Barber, D.L. The glycolytic enzyme phosphofructokinase-1 assembles into filaments. *J. Cell Biol.* **2017**, *216*, 2305–2313. [CrossRef] [PubMed]
80. Curci, P.L.; Cigliano, R.A.; Zuluaga, D.L.; Janni, M.; Sanseverino, W.; Sonnante, G. Transcriptomic response of durum wheat to nitrogen starvation. *Sci. Rep.* **2017**, *7*, 1–14. [CrossRef] [PubMed]
81. Kamada, T.; Nito, K.; Hayashi, H.; Mano, S.; Hayashi, M.; Nishimura, M. Functional differentiation of peroxisomes revealed by expression profiles of peroxisomal genes in Arabidopsis thaliana. *Plant Cell Physiol.* **2003**, *44*, 1275–1289. [CrossRef] [PubMed]
82. Reumann, S.; Ma, C.; Lemke, S.; Babujee, L. AraPerox. A database of putative Arabidopsis proteins from plant peroxisomes. *Plant Physiol.* **2004**, *136*, 2587–2608. [CrossRef] [PubMed]
83. Massoumi, M.; Krens, F.A.; Visser, R.G.; De Klerk, G.J.M. Etiolation and flooding of donor plants enhance the capability of Arabidopsis explants to root. *Plant Cell Tissue Organ Cult.* **2017**, *130*, 531–541. [CrossRef]
84. Suárez, E.; Alfayate, C.; Pérez-Francés, J.F.; Rodríguez-Pérez, J.A. Structural and ultrastructural variations in in vitro and ex vitro rooting of microcuttings from two micropropagated Leucospermum (Proteaceae). *Sci. Hortic.* **2018**, *239*, 300–307. [CrossRef]
85. Kim, D.; Langmead, B.; Salzberg, S.L. HISAT: A fast spliced aligner with low memory requirements. *Nat. Methods* **2015**, *12*, 357–360. [CrossRef] [PubMed]
86. Pertea, M.; Pertea, G.M.; Antonescu, C.M.; Chang, T.C.; Mendell, J.T.; Salzberg, S.L. StringTie enables improved reconstruction of a transcriptome from RNA-seq reads. *Nat. Biotechnol.* **2015**, *33*, 290–295. [CrossRef] [PubMed]